Research on Engineering Structures & Materials
www.jresm.org
Research Group

Research Article

Enhanced properties of recycled ceramic fine aggregates via cement and sodium bicarbonate treatment: Experimental study, microstructure analysis and modeling

Tarek Zeribi [1,3,a], Tarek Djedid [*,2,3,b], Mohamed Zohaïr Kaab [1,3,c], Tahar Zerig [4,d], Brahim Athamnia [5,e], Noureddine Hamdi [6,f]

[1]*Unit for the development of renewable energy in arid areas (UDERZA), Algeria*
[2]*Laboratory of exploitation and valorization of Saharan energy resources "LEVRES", Faculty of Exact Sciences, University of El Oued, 39000, Algeria*
[3]*Department of Hydraulic and Civil Engineering, Faculty of Technology, University of El Oued, 39000, Algeria*
[4]*Laboratory LGCH, University 8 May 1945 Guelma, Algeria*
[5]*Laboratory of Applied Civil Engineering (LGCA), Department of Civil Engineering, Echahid Cheikh Larbi Tebessi University, Tebessa 12002, Algeria*
[6]*Higher Institute of water sciences and Techniques, University of Gabès, 6072, Zrig, Tunisia*

Article Info

Article History:

Received 08 Jan 2026

Accepted 13 Mar 2026

Keywords:

Recycled ceramic fine aggregates;
Cement and sodium bicarbonate treatment;
Physical properties;
Microstructural analysis;
Response surface methodology

Abstract

The aim of this contribution is to improve the physical characteristics of waste ceramic fine aggregates (WCFA) which have a particle size of 0 to 5 mm through surface chemical treatment, while diagnosing: bulk density, water absorption, and apparent porosity. The impregnation protocol involves applying a solution of cement (C) and sodium bicarbonate (SB) to the aggregate surface at the following concentrations (C: 2% and 4%; SB: 2%, 4%, 6% and 8%) and immersion durations of 12, 24, 48, and 72 hours. The microstructural examination consisting of X-ray diffraction (XRD), Fourier transform infrared spectroscopy (FTIR), and scanning electron microscopy (SEM) with Energy Dispersive Spectroscopy (EDS) was used to determine the physical effectiveness of this treatment to the WCFA accurately. A design of experiments dependent on response surface methodology was created to find the best treatment conditions. Results showed that the sample (4C4SB24H) increased its bulk density by about 11.5% and reduced water absorption by immersion and apparent porosity by 41.3% and 47.9% respectively as compared with the untreated control sample. A normal new calcite distribution was observed, which very well demonstrated the maximum reduction of surface pore spaces, thus confirming the quality of the chosen sample one more time. The statistical interpretation via Box-Behnken (BBD) suggested that the proposed model was very effective since the maximum error was only 7%.

1. Introduction

The fast industrial development in developed countries has made waste management problems even worse. The issue is caused by environmental and economic pressures together with the depletion of natural resources [1]. Waste recovery has been made a necessity in the course of the sustainable development strategy. This method is highly pertinent to the construction industry in which the use of concrete must be limited to impacts that are not harmful to nature [2]. Various nations such as England, China, and Spain have stringent laws that govern the use of recycled

*Corresponding author: tarek-djedid@univ-eloued.dz
[a]orcid.org/ 0009-0008-5243-6048; [b]orcid.org/0000-0002-1249-156X; [c]orcid.org/0000-0003-3572-2890; [d]orcid.org/0000-0002-6713-4666; [e]orcid.org/ 000-0003-0525-3499; [f]orcid.org/0000-0002-2223-2115
DOI: http://dx.doi.org/10.17515/resm2026-1461ma0108rs

aggregates for concrete production. These laws promote aggregates primarily made of crushed concrete and natural stone that are stuck together with mortar [3–5]. On the contrary, Germany and the Netherlands have gone a step further and have set lax rules permitting the blending of recycled aggregates from concrete, stone, ceramics, masonry, asphalt, or any other mineral materials [6,7]. The application of recycled ceramic aggregates from the sanitary industry in concrete is an area of research that is growing very fast due to the absence of specific standards for their reuse [8]. A number of studies have pointed out its potential as an active additive to cement by taking advantage of its pozzolanic activity to enhance the durability and mechanical performance of materials [9–14]. Other studies have shown that they can be effective natural aggregate partial substitutes, and the findings are quite promising depending on the substitution rates [15–23]. Ceramic waste, primarily from defective items or manufacturing scraps, is produced every day and increasingly challenging for the producers [24,25]. Poor waste management can cause significant environmental impacts, so it is essential for the construction sector to come up with eco-friendly recovery options [26]. Treatment facilities for construction and demolition waste (CDW) have shown to be cost-effective [27], still There are technical issues that need to be solved before these materials can be used as a substitute for natural aggregates. The mechanical behavior of the resulting concrete was a significant impact [28–30], the workability at the same water/cement (w/c) ratio has already been mentioned as an important factor [31], and the durability of concrete has been also the subject of discussion [32]. Recycled aggregates have been carefully chosen in some research works to give the same or better results [33], while their pre-treatment, washing, for instance, to remove fine fractions with high soluble sulfate content and water absorption was also proved to be very effective [34–36], besides, the cement with the incorporation of mineral admixtures was used [37,38]. Ceramic aggregates ensure an excellent level of resistance while still being very effective in heat and having a very low thermal expansion coefficient [39]. Replacing natural aggregates with them in concrete is the very process that helps to benefit the environment by managing the industrial waste [40,41]. Recent experiments by D. J. Anderson et al. [42], A. V. Alves et al. [43], C. Medina et al. [44], L. A. Pereira-de-Oliveira et al. [45], M. O'Farrell et al. [46], J. Silva et al. [47], have studied the introduction of ground sanitaryware and earthenware ceramics into building materials with the focus being on their usability as alternative raw materials for mortar and concrete composition. This study has demonstrated the bright potential of this waste as a source of materials with good mechanical and physical properties, thus contributing to the cause of sustainable development. Different methods of treatment have been investigated to enhance the recycling aggregate's resistance to water absorption, among which A. Barbudo et al. [48], established that recycled concrete aggregates (RCA) could substitute for natural aggregates in a maximum proportion of 20% without causing any reduction in compressive strength, and a substitution of 100% is possible when a water reducer is mixed up to offset these high absorption levels, this approach focuses primarily on adjusting the mix composition by adding water-reducing admixtures to maintain mechanical performance. Similarly, D. Matias et al. [49], pointed out that the addition of a superplasticizer partially compensates for the loss of workability and strength due to high water absorption, while improving the compactness and mechanical performance of concrete made from recycled concrete aggregates (RCA). these works brought up the topic of using water-reducing admixtures, while K. K. Sagoe-Crentsil et al. [50], have shown that industrial processing of recycled concrete aggregates (RCA) produces more spherical and smoother particles, and that pre-saturation of these aggregates in water improves the workability of concrete without significantly reducing its compressive strength at 28 days. Likewise, J. García-González et al. [51] demonstrated the feasibility of pre-saturating recycled aggregates in order to limit their water absorption. Immersion for 3 to 5 minutes significantly improves the workability of the concrete (plastic to fluid consistency), with limited loss of compressive strength (≈ 11–13%), These studies focused on the method of pre-saturation of aggregates. Some studies have examined the possibility of applying various chemical treatments to recycled aggregates. For example, S. Ismail and M. Ramli [52] have shown that surface treatment of recycled aggregates, combining mild acid attack to remove mortar residues and impregnation with a cementitious solution to reduce porosity, significantly improves their physical and mechanical properties, enabling the concrete to achieve better strength and reduced shrinkage. V. Spaeth and A. Djerbi Tegguer [53] showed that polymer treatments applied to recycled aggregates form a protective film in the porous network,

significantly reducing water absorption and strengthening the cement matrix. A. M. Grabiec et al. [54] showed that calcium carbonate biodeposition effectively reduces the water absorption of recycled aggregates, with a notable improvement for fine fractions (≈30–35%). Confirmed by SEM observations. However, the proposed methods, such as carbonation and chemical waterproofing, have significant limitations, including prolonged reaction times and incompatibility with sustainable development requirements. The very slow and difficult alternative of bio-deposition of calcium carbonate, which has been studied by V. Achal et al. [55] and Q. Chunxiang et al. [56], still holds promise but is difficult to reconcile with the working conditions of construction sites. Some previous studies have produced contradictory results in respect to the physical properties of ceramic waste, drawing attention to large difference which varies depending on its origin, kind and manufacturing methods. For instance, Kwok Wei Shah and Ghasan Fahim Huseien [57] analyzed white ceramic tile waste, measuring a real density of 2.38 g/cm^3, a visual density of 1.450 g/cm^3, and a water absorption of 1.3%. On the other hand, Abadou Y et al. [58] reported values of 2.288 g/cm^3 for the real density, 1.212 g/cm^3 for the visual density, and a water absorption of as high as 30% for ceramic sanitary waste. Derrick J. Anderson et al. [42] have mentioned a real density of 2.263 g/cm^3 and a water absorption of 5.5%, while D. Tavakoli et al. [28] found 2.6 g/cm^3, 1.750 g/cm^3 and 2% for another variety of ceramics. This evidence, supported by other research works [59–68], reveals the fundamental differences in the features of ceramic waste according to its source and chemical composition. In order to improve the physical characteristics of recycled aggregates, particularly their water absorption, for use in concrete or cementitious matrices, several treatment methods have been developed. The results obtained vary depending on the nature of the aggregates and the technique used. Mistri A et al. [65] conducted a comparative study of different treatments aimed at improving the properties of recycled aggregates (RCA). They observed a reduction in water absorption of 48.62% for a treatment combining mechanical grinding and soaking, 18.82% for autogenous cleaning, 19.36% for treatment with an acid solution (0.1 M HCl for 3 days), 4.23% for simple acid treatment (HCl), 9.47% for thermal treatment at 350°C, and 2.03% for chemical treatment with acetic acid ($C_2H_4O_2$). García-González J et al. [69] studied the improvement in the quality of mixed and ceramic recycled aggregates through calcium carbonate biodeposition and reported a decrease in water absorption of 46% (TEC-REC samples), 41% (ANTWERP) and 16% (BIERZO). Mareeswari Andal N et al. [70] analyzed the effect of chemical treatment on recycled fine aggregates and found a reduction in water absorption of 12.48%, 38.31%, and 54.35% for HCl concentrations of 0.1 M, 0.4 M, and 0.7 M, respectively. Other studies [54,71,72] have also explored different treatment techniques, but have mainly focused on the mechanical and physical properties of concrete after incorporation of the treated aggregates, rather than on the in-depth characterization of the aggregates themselves. With regard to treatment using a suspension of cement and sodium bicarbonate, to the best of our knowledge, only one study, conducted by Phan et al. [73] , has been identified. The authors studied effect of recycled coarse aggregate treatment using cement and sodium bicarbonate slurry on compressive strength of hardened concrete and reported water absorption of RCA of 3.3%, corresponding to an improvement of 18.51%. The cement mainly containing tricalcium silicate (C_3S) and dicalcium silicate (C_2S) reacts with sodium bicarbonate ($NaHCO_3$) through several stages. The hydration of cement consists of water reacting with cement to produce calcium hydroxide ($Ca(OH)_2$) and other hydration products, as illustrated in chemical Eqs. (1)-(2):

$$2C_3S + 6H_2O \rightarrow CSH + 3Ca(OH)_2 \quad (1)$$

and

$$2C_2S + 4H_2O \rightarrow CSH + Ca(OH)_2 \quad (2)$$

Subsequently, calcium hydroxide and sodium bicarbonate interact to produce calcium carbonate ($CaCO_3$), sodium carbonate (Na_2CO_3), and water as per the following chemical Eq. (3):

$$Ca(OH)_2 + 2NaHCO_3 \rightarrow CaCO_3 + Na_2CO_3 + 2H_2O \quad (3)$$

Calcium carbonate ($CaCO_3$) is therefore produced, which has the potential to occupy the voids of recycled aggregates, enhance their strength and durability and also decrease their porosity and water absorption.

The research was based on the only existing study on the treatment of recycled aggregates using a suspension of cement and sodium bicarbonate. We aimed to optimize the treatment of fine aggregates from ceramic waste using a combination of cement and sodium bicarbonate suspension, varying their concentrations along with the immersion durations, while carrying out an in-depth characterization of this type of aggregate. The physical, structural, and morphological analyses were performed to evaluate the impact of these parameters and to find the best conditions for enhancing the density of aggregates with minimum porosity and water absorption. To uncover the quantitative relationship among the treatment variables and the WCFA properties, a statistical modeling strategy was employed, which is based on response surface modeling (RSM) and Box-Bennkin design of experiments (BBD).

2. Methods

2.1 Materials

2.1.1 Waste Ceramic Fine Aggregates (WCFA)

The fine ceramic aggregate waste (WCFA) was produced by grinding ceramic floor tiles from the SARL CONFORT CERAM factory located in El Hadjeb, Biskra, Algeria. This waste is formed by red ceramics that are either from defective products or manufacturing residues. It is a very durable material that offers the highest resistance against both chemical and physical degradation [16,25].

Only unglazed tiles, which are purely fired biscuits, were taken for the study so that the physical properties such as porosity, water absorption, and density could be examined. The lack of the glaze layer (which is an impermeable layer) is taken as the most cautious case in this research.

Fig. 1. Toothed jaw crusher used for crushing aggregates

Waste ceramics were subjected to crushing by a toothed jaw crusher calibrated with the aim of fine aggregate production Fig. 1. This type of crusher, for the most part, is utilized to produce end products for aesthetic applications in the construction of marble powder. The machine, in this case, works by making the materials go through the two jaws, one of which is stationary while the other is free to move. The materials are pressed, and the teeth of the jaws enhance the compressive force and create more pressure points which result in more efficient crushing and also controlled particle size reduction. This kind of crusher is mostly used in the mining industry to deal with hard and rough materials like rocks, ores, and even building materials. The larger aggregates were then processed through a 5 mm sieve to get Waste Ceramic Fine Aggregates (WCFA). The measuring of the sieve was done according to the NF EN 933-1 standard [74]. A histogram showing the size

distribution of the aggregate obtained is presented in Fig. 2. The high value of the Coefficient of Uniformity (Cu = 12.32) implies that there was a significant variation in the sizes of the particles, and the Coefficient of Curvature (Cc = 1.59) is supportive of a fairly high and good quality distribution of particles. The fineness modulus, being equal to 3.51, shows that WCFA is coarser than standard sand used in construction with regard to the latter's finer particle size distribution. But then, the uniformity of the particle size distribution may help in the incorporation of WCFA into particular formulations of building materials with the possibility of alterations made to the performance of the product to be optimized.

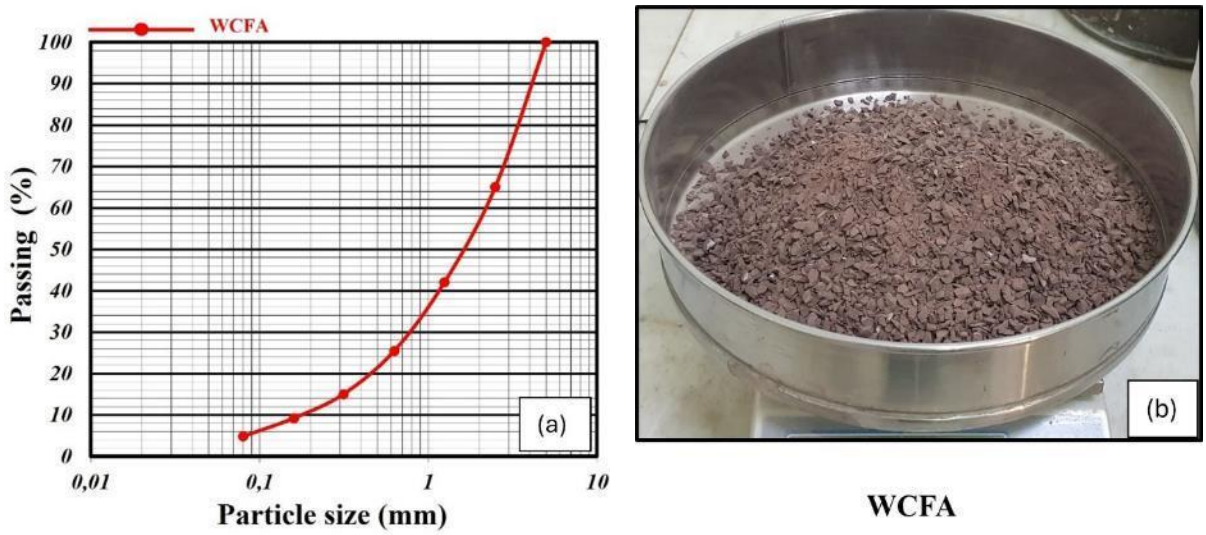

Fig. 2. Toothed jaw crusher used for crushing aggregates

2.1.2 Cement (C) and sodium bicarbonate (SB)

The cement that was utilized is CEM I - 42.5N SR3 LH (sulfate-resistant with low heat of hydration), which complied with the Algerian standard NA442-2013, having a clinker content of 95%-100% and containing 0-5% of additional components. Supplied by Biskria Ciment. The main phases of clinker, namely dicalcium silicate (C_2S) and tricalcium silicate (C_3S), react with water according to Eqs. (1)-(2), producing calcium hydroxide ($Ca(OH)_2$). The latter then reacts with sodium bicarbonate ($NaHCO_3$) to form calcium carbonate ($CaCO_3$), as illustrated in Eq. (3).

Sodium bicarbonate ($NaHCO_3$) purity 100.3% min was supplied by EDEN-LABO SARL.

2.2 Sample Preparation

WCFA were crushed and sieved to obtain a uniform granulometry, with particle sizes ranging from 0.063 mm to 4 mm. Aggregates smaller than 4 mm were washed through a 0.063 mm sieve to remove irrelevant fine particles [58,74,75]. The aggregates were then air-dried under controlled laboratory conditions (20 ± 2 °C and 50 ± 5% relative humidity), for 14 days until a constant mass was obtained [65,70,73,74,75]. The basic properties of the fine ceramic waste aggregates (WCFA) before treatment were evaluated to establish a comparative basis for the processed samples. The results obtained show an absolute density of 2.3 g/cm^3, a bulk density of 1.103 g/cm^3, a water absorption of 6.046% and an apparent porosity of 14.32%. These data indicate that the aggregates studied have a high porosity and significant absorption capacity. Previous studies have reported variable characterizations of crushed ceramic waste [29,43,58–65,66–68,73].

2.3 Sample Treatment

After crushing, treatment solutions were prepared by dissolving cement and sodium bicarbonate in distilled water under magnetic stirring for 5 minutes. During treatment, samples were kept under gentle agitation to prevent sedimentation and ensure uniform exposure to the solution.

WCFA were treated to examine the effect of cement and NaHCO3 suspensions on their porosity and water absorption. Samples of 1 kg were prepared for each treatment [73]. WCFAs were immersed

in a solution comprising various amounts of cement and $NaHCO_3$ (Fig. 3.), with varying immersion durations, as shown in Table 1.

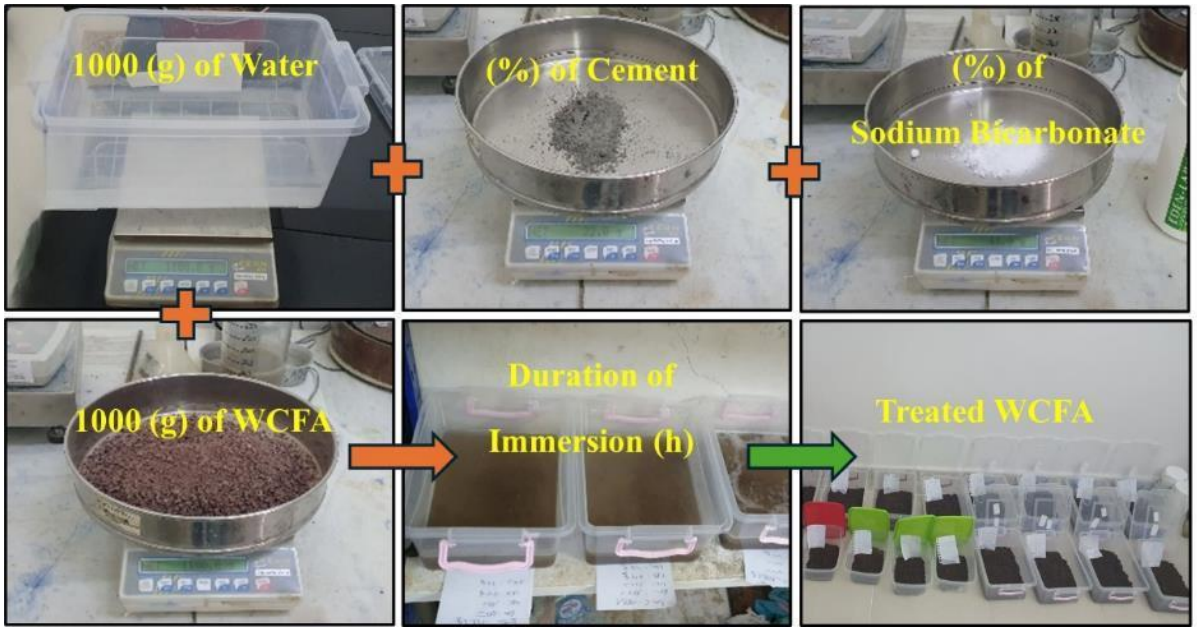

Fig. 3. Photos illustrating WCFA treatment process

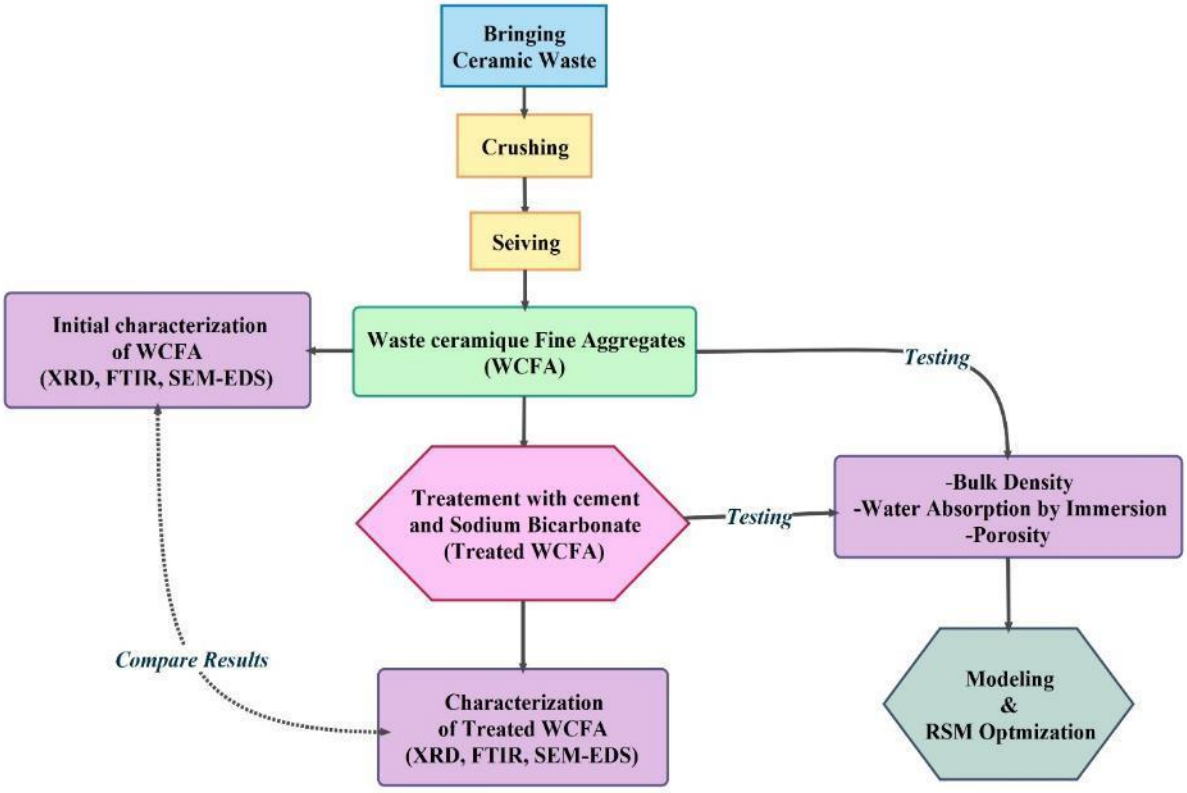

Fig. 4. Experimental procedure

Table 1. Mix composition and experimental conditions for processing recycled aggregates

Symbol	Slurry concentration		Components				Immersion duration (hours)
	C (%)	NaHCO3 (%)	C (%)	NaHCO3 (g)	W (g)	RCA (g)	
0C0SB0H	0	0	0	0	0	0	0
2C2SB12H	2	2	20	20	1000	1000	12
2C4SB12H	2	4	20	40	1000	1000	12
2C6SB12H	2	6	20	60	1000	1000	12
2C8SB12H	2	8	20	80	1000	1000	12
4C2SB12H	4	2	40	20	1000	1000	12
4C4SB12H	4	4	40	40	1000	1000	12
4C6SB12H	4	6	40	60	1000	1000	12
4C8SB12H	4	8	40	80	1000	1000	12
2C2SB24H	2	2	20	20	1000	1000	24
2C4SB24H	2	4	20	40	1000	1000	24
2C6SB24H	2	6	20	60	1000	1000	24
2C8SB24H	2	8	20	80	1000	1000	24
4C2SB24H	4	2	40	20	1000	1000	24
4C4SB24H	4	4	40	40	1000	1000	24
4C6SB24H	4	6	40	60	1000	1000	24
4C8SB24H	4	8	40	80	1000	1000	24
2C2SB48H	2	2	20	20	1000	1000	48
2C4SB48H	2	4	20	40	1000	1000	48
2C6SB48H	2	6	20	60	1000	1000	48
2C8SB48H	2	8	20	80	1000	1000	48
4C2SB48H	4	2	40	20	1000	1000	48
4C4SB48H	4	4	40	40	1000	1000	48
4C6SB48H	4	6	40	60	1000	1000	48
4C8SB48H	4	8	40	80	1000	1000	48
2C2SB72H	2	2	20	20	1000	1000	72
2C4SB72H	2	4	20	40	1000	1000	72
2C6SB72H	2	6	20	60	1000	1000	72
2C8SB72H	2	8	20	80	1000	1000	72
4C2SB72H	4	2	40	20	1000	1000	72
4C4SB72H	4	4	40	40	1000	1000	72
4C6SB72H	4	6	40	60	1000	1000	72
4C8SB72H	4	8	40	80	1000	1000	72

2.4 Experimental procedure

Physical testing of fine ceramic aggregates follows the methodology shown in Fig. 4. illustrates the sequence of experimental steps, from sample preparation to evaluation of the physical properties of the aggregates and their modeling using the Response Surface Method (RSM).

2.4.1 Bulk Density and Absolute Density

The WCFA bulk density (ρ_a) was measured as per ASTM C29/C29M [76] standard method using the shoveling procedure. The experiment was carried out in three repetitions for each test to confirm the accuracy and reproducibility of results. The total mass of the test sample was reduced at the temperature of 110 ± 5°C until no further loss of weight was observed to eliminate the effect of moisture left in the sample. A test mold, which was of known volume, was used for the test and the volume was previously validated according to the standard requirements to assure the accuracy of the calculation. The aggregate was then filled in the container without compacting it by pouring gently using a shovel from a height of no more than 50 mm above the edge of the container. To prevent segregation of the particles care was taken. The excess was then cut off using a ruler or

fingers, to equalize the heights of the surface protrusions and fill up the voids. Thereafter, the bulk density was computed using the following Eq. (4):

$$\rho_a = \frac{(G-T)}{V} \tag{4}$$

where, G is the mass of the filled container (g), T is the mass of the empty container (g), V is the volume of the container (cm^3) [76]. All measurements were recorded to ±0.01 g precision using a calibrated analytical balance. The absolute density (ρs) corresponds to the mass per unit volume of the material constituting the processed WCFA, without considering internal or intergranular voids. It is determined in accordance with ASTM C128 [72] with three repetitions of each test and by the following method: a graduated cylinder is filled with an initial volume of water (V_1), then a dry sample of mass (M) is added. After removing air bubbles, the new volume (V_2) is measured. The absolute density is obtained by the Eq. (5):

$$\rho_s = \frac{M}{(V_2 - V_1)} \tag{5}$$

where, M is the mass of dry aggregate (g), V1 is the initial volume of water (cm^3), V2 is the final volume after immersion of aggregate (cm^3) [75].

2.4.2 Water Absorption by Immersion

The water absorption test by immersion was conducted according to ASTM C128 [72], , with each measurement carried out three times. The samples underwent drying in an oven at 110 ± 5°C to obtain a constant weight (weight variation Δm < 0.1 %). The next step was to submerge the samples in water for 24 hours. Later on, the samples were allowed to drain, and then placed on a wet cloth for 15 to 20 minutes to reduce the water loss. The samples were then in their saturated surface dry (SSD) condition, and their weight was measured and recorded as S. After that, the samples were dried again in an oven at 110 ± 5 °C until constant weight was reached, and this weight was referred to as dry weight A. Water absorption was calculated to an accuracy of 10^{-3} g by applying Eq. (6):

$$Absorption(\%) = 100 \times \frac{(S-A)}{A} \tag{6}$$

where, S is the mass of the saturated surface dry (SSD), A is the mass of the dry sample after oven drying [75].

2.4.3 Apparent Porosity

The ultrafine particles in each WCFA sample with an initial mass of 1 kg are removed by washing through a 0.063 mm sieve. The method for measuring apparent porosity ASTM C20 [73] is utilized for the tests, which are repeated three times each. To start, the sample is placed in an oven at 110 ± 5 °C for drying until its weight becomes constant, then it is weighed (D) in order to exclude moisture from the material's pores. Subsequently to the drying process, the sample is placed in boiling water for two hours to ensure complete saturation of the pores. Following this, the sample is left in water for a minimum of 12 hours, then it gets removed and it gets wiped for getting a saturated dry surface (SSD). Now the saturated weight (W) is measured. The volume of the sample is obtained by using Eq. (7):

$$V(cm^3) = W - S \tag{7}$$

where, W stands for the weight of the specimen at the time of the saturated surface-dry (SSD) state, S hydrostatic weight represents mass of the sample, determined by suspending the sample in water from a thin wire operated by metal wire [77]. It is from the value of W and D that the calculated value of apparent porosity is evaluated by the result of the analysis as outlined in Eq. (8):

$$Porosity(\%) = 100 \times \frac{(W-D)}{V} \tag{8}$$

where, W is the mass of sample saturated surface dry (SSD) (g), D is the mass of sample dry (g), V is the volume of the test specimens (cm^3), as defined in Eq. (7). [77].

2.5 Microstructural Analyses

2.5.1 Fourier Transform Infrared Spectroscopy (FTIR) Analysis: Identification of mineral phases

An FTIR analysis for determining the mineral phases of the recycled fine ceramic aggregate was executed in order to examine the impact of chemical treatment on the degree of crystallinity of calcite ($CaCO_3$). The recordings of the spectra were made in the range of 4000–400 cm^{-1}, thus making it possible to observe the progress of the carbonate aggregates and simultaneously keep track of the treatment-induced structural changes.

2.5.2 X-ray Diffraction (XRD) Analysis: Evolution of Mineral Phases after Treatment

The fine ceramic aggregate (WCFA) was characterized for their mineralogical phases using x-ray diffraction (XRD) as well as observing the evolution of the vesicles before and after treatment with a suspension of cement and sodium bicarbonate. Major minerals can be identified using non-destructive techniques and relative estimates of their abundances, as a result, the study provided a comprehensive picture of the chemical reactions taking place during the treatment process and their influence on the microstructure as well as the properties of the aggregate being used.

2.5.3 Scanning Electron Microscopy (SEM) and Energy Dispersive Spectroscopy (EDS)

The morphology of the treated aggregate was scrutinized through scanning electron microscopy (SEM), which allowed changing in surface structure and the deposition, especially calcium carbonate ($CaCO_3$), which is a crucial raw material for enhancing the aggregate's physical properties, to be observed.

Moreover, EDS helped in confirming the elemental composition of the sample surfaces as well as the presence of Ca^{2+} through the technique that was excellent in this study which enabled the ascertainment of the proportions of chemical elements that were present and validation of the occurrence of calcium ions (Ca^{2+}), which also play an essential role in the crystallization of calcium carbonate ($CaCO_3$).

2.6 Response Surface Analysis and Experimental Design

The software Design-Expert (ver. 13.0.5.0) was used to improve the precision of experimental results and to create graphs showing the treatment effects. The different concentrations of cement and sodium bicarbonate were tested to determine the best treatment conditions.

The Box-Behnken design (BBD), the most popular method for studying the influence of three independent factors, namely cement content (%C), sodium bicarbonate content (%SB), and immersion duration (ID in hours), was employed for the layout of the experiments. We chose the Box-Behnken model as it is very productive in studying the linear, quadratic and interaction effects among factors, to reduce the number of experiments and eliminate limit cases and thereby provide a viable tradeoff between statistical precision and experimental economy.

Response surface model (RSM) was applied to analyze data with focus on main variables as bulk density, water absorption, and apparent porosity. By utilizing a modified second-order polynomial (Eq. (9)), [78–82], the connection between the factors and the responses was improved. The resulting equation is as follows:

$$Y = \beta_o + \sum_{i=1}^{k} \beta_i X_i + \sum_{i<j}^{k} \beta_{ij} X_i X_j + \sum_{i=1}^{k} \beta_{ii} X_i^2 \quad (9)$$

where, Y is the response, Xi represents the independent variables (experimental factors), β0 is the intercept, βi, βij, and βii are the coefficients of the linear, interactive, and quadratic terms respectively [78–82].

Table 2 shows the factors and levels used to design the experiment. The variables were encoded in three categories: the minimum value was represented by (-1), the median value was represented by (0), and the maximum value was represented by (+1). Different combinations of variables (total of 33 experiments) were tested with this methodology, as listed in Table 3.

Table 2. Factors and code levels of RSM

Factors	Coded	Levels of code		
		Min (-1)	Medium (0)	Max (1)
Cement (%)	A	0	2	4
Sodium Bicarbonate (%)	B	0	4	8
Immersion Duration (h)	C	0	24	72

3. Results and Discussion

3.1 Effects of Treatments on Physical Properties

The results, which are illustrated in Table 3, are indicative of the significant impacts both of cement slurry and $NaHCO_3$ treatments on physical properties of WCFA. The physical properties of the samples, such as bulk density, water absorption, and apparent porosity, were used to assess the impact of each independent variable (cement composition, sodium bicarbonate concentration, and immersion duration). The assessment results have been compiled and charted in Fig. 5.

Table 3. Physical and chemical properties of treated samples

Sample No.	Notation	Cement (%)	Sodium Bicarbonate (%)	Immersion Duration (h)	Absolute Density (g/cm^3)	Bulk Density (g/cm^3)	Absorption by Immersion (%)	Apparent porosity (%)
1	0C0SB0H	0	0	0	2.3	1.1030 ± 0.0016	6.046 ± 0.352	14.32 ± 0.79
2	2C2SB12H	2	2	12	2.3	1.1611 ± 0.0049	4.783 ± 0.132	10.72 ± 0.41
3	2C4SB12H	2	4	12	2.3	1.1767 ± 0.0080	4.047 ± 0.119	9.93 ± 0.34
4	2C6SB12H	2	6	12	2.3	1.1894 ± 0.0031	3.833 ± 0.117	9.61 ± 0.33
5	2C8SB12H	2	8	12	2.3	1.1896 ± 0.0061	4.243 ± 0.095	9.72 ± 0.31
6	4C2SB12H	4	2	12	2.3	1.1787 ± 0.0065	4.495 ± 0.147	10.74 ± 0.41
7	4C4SB12H	4	4	12	2.3	1.1946 ± 0.0025	3.906 ± 0.133	9.75 ± 0.40
8	4C6SB12H	4	6	12	2.3	1.2046 ± 0.0030	3.817 ± 0.124	9.67 ± 0.37
9	4C8SB12H	4	8	12	2.3	1.2053 ± 0.0065	3.774 ± 0.126	9.59 ± 0.39
10	2C2SB24H	2	2	24	2.3	1.1978 ± 0.0049	4.793 ± 0.136	9.55 ± 0.32
11	2C4SB24H	2	4	24	2.3	1.2011 ± 0.0040	4.283 ± 0.132	8.57 ± 0.31
12	2C6SB24H	2	6	24	2.3	1.2158 ± 0.0053	4.163 ± 0.137	8.8 ± 0.33
13	2C8SB24H	2	8	24	2.3	1.2211 ± 0.0029	4.443 ± 0.142	8.89 ± 0.34
14	4C2SB24H	4	2	24	2.3	1.2040 ± 0.0066	4.357 ± 0.124	9.65 ± 0.41
15	4C4SB24H	4	4	24	2.3	1.2303 ± 0.0044	3.549 ± 0.092	7.45 ± 0.22
16	4C6SB24H	4	6	24	2.3	1.2307 ± 0.0051	3.572 ± 0.098	8.45 ± 0.39
17	4C8SB24H	4	8	24	2.3	1.2291 ± 0.0010	3.712 ± 0.112	8.49 ± 0.36
18	2C2SB48H	2	2	48	2.3	1.1891 ± 0.0014	4.216 ± 0.096	7.51 ± 0.32
19	2C4SB48H	2	4	48	2.3	1.2055 ± 0.0068	4.309 ± 0.127	7.75 ± 0.31
20	2C6SB48H	2	6	48	2.3	1.2091 ± 0.0022	4.362 ± 0.109	7.66 ± 0.33
21	2C8SB48H	2	8	48	2.3	1.2093 ± 0.0038	4.497 ± 0.124	8.98 ± 0.34
22	4C2SB48H	4	2	48	2.3	1.1870 ± 0.0071	4.431 ± 0.141	8.49 ± 0.36
23	4C4SB48H	4	4	48	2.3	1.2029 ± 0.0069	4.223 ± 0.111	7.96 ± 0.28
24	4C6SB48H	4	6	48	2.3	1.2111 ± 0.0062	4.217 ± 0.126	7.82 ± 0.34
25	4C8SB48H	4	8	48	2.3	1.2037 ± 0.0031	4.219 ± 0.126	9.19 ± 0.36
26	2C2SB72H	2	2	72	2.3	1.1513 ± 0.0052	3.702 ± 0.109	8.49 ± 0.33
27	2C4SB72H	2	4	72	2.3	1.1729 ± 0.0011	3.717 ± 0.126	8.23 ± 0.35
28	2C6SB72H	2	6	72	2.3	1.1741 ± 0.0042	3.695 ± 0.109	8.47 ± 0.31
29	2C8SB72H	2	8	72	2.3	1.1754 ± 0.0051	3.949 ± 0.122	9.54 ± 0.40
30	4C2SB72H	4	2	72	2.3	1.1469 ± 0.0069	3.755 ± 0.117	8.64 ± 0.37
31	4C4SB72H	4	4	72	2.3	1.1602 ± 0.0071	3.567 ± 0.103	7.74 ± 0.33
32	4C6SB72H	4	6	72	2.3	1.1592 ± 0.0042	3.551 ± 0.096	7.54 ± 0.31
33	4C8SB72H	4	8	72	2.3	1.1496 ± 0.0055	3.932 ± 0.120	9.01 ± 0.38

As shown in Table 3, the absolute density of all specimens remained steady at 2.30 g/cm^3, with low variability as the standard deviation is ±0.001 g/cm^3, the remarkable degree of density homogeneity ascertains that crushing and sieving of WCFA materials generated almost homogenous granules. On the contrary, using cement suspension together with sodium

bicarbonate ($NaHCO_3$) caused remarkable changes in bulk density, water absorption, and apparent porosity. These changes are indicative of the fine aggregate's structural and chemical alterations that have been made without affecting their absolute density to a large extent.

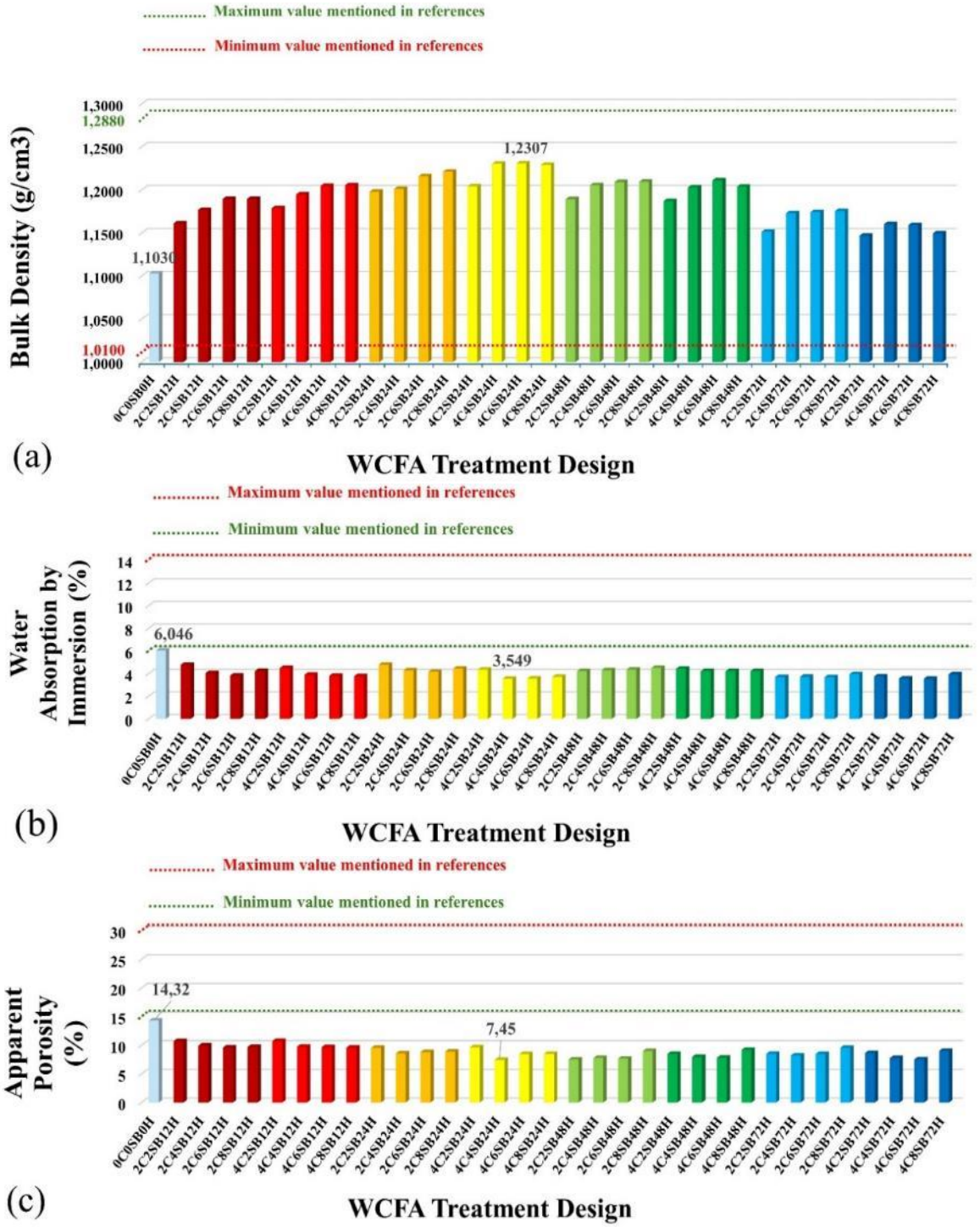

Fig. 5. Characteristics of the treated fine aggregate: (a) bulk density, (b) water absorption, and (c) apparent porosity

The samples that underwent treatment and were immersed for 12 hours exhibited a significant enhancement in their performance when compared to the control sample (0C0SB0H), signified by a bulk density of 1.1030 g/cm^3, an immersion water absorption rate of 6.046%, and an apparent porosity of 14.32%. Literature data shows that fine aggregates obtained from crushing floor ceramic waste have bulk density ranging from 1.0100 to 1.2880 g/cm^3, water absorption between 6.00% and 14.00%, and apparent porosity from 15.00% to 30.00% [18,42,58,60,62,67,83,84] Fig. 5.

Sample 2C8SB12H attains a maximum bulk density of 1.1896 g/cm^3, a water absorption of 4.243%, and an apparent porosity of 9.72%. The figures present an enhancement of 7.85% in density, 29.8% decrease in water absorption, and 32.1% decline in apparent porosity when compared to the baseline sample 0C0SB0H, thus indicating the efficacy of the treatment from the start of immersion.

The effects of physical properties improvement by the dissolution of cement and $NaHCO_3$ in the mixtures or the prolongation of the immersion time were actually seen with increasing concentration. The 4C6SB24H specimen exhibited noteworthy characteristics such as a density of 1.2307 g/cm^3, a water absorption percentage of 3.572%, and an apparent porosity of 8.45% following a 24-hour immersion period. When the results were compared to those of the control sample (0C0SB0H), the differences were the following: 11.6% increase in bulk density, 40.9% decrease in water absorption, and 41.0% reduction in apparent porosity corresponding to a considerable densification of the material and significant minimization of the internal voids all patterns of the same.

Sample 4C4SB24H exhibited a performance that was impressive, as it managed to achieve a bulk density of 1.2303 g/cm^3, water absorption of 3.549%, and apparent porosity of 7.45%. With 11.5% higher bulk density, 41.3% less water absorption, and 47.9% less apparent porosity. The mentioned improved properties apply not only to the durability of fine aggregates but also to their adaptability to the various environmental situations existing in construction uses, which make them very prominent characteristics. The results support the ones presented by Phan et al. [73] who also communicated a similar density variation and porosity reduction while dealing with cementitious mixtures supplemented with sodium bicarbonate. The mixtures containing 4% of cement, 4% of sodium bicarbonate.

3.2 Structural modification of Treated WCFA

3.2.1 Analysis by Fourier Transform Infrared (FTIR) Spectroscopy: Mineral Phases

Fig. 6. shows the mineral phases identified by FT-IR spectroscopy, in a wavenumber range from 4000 to 400 cm-^{1}. Characteristic carbonate bands, particularly for calcite ($CaCO_3$), are observed at ~711, 743-776, and 792-793 cm-^{1}. These correspond to the out-of-plane deformation vibrations (ν_4) of the carbonate group (CO_3^{2-}), indicating stable crystallization of $CaCO_3$ after treatment [30,85,86]. Silicates, mostly in quartz form (SiO_2), were identified by peaks at 553, 562, 569, and 580 cm-^{1}, which are attributed to bending vibrations Si-O. Also, peak at 1008 cm-^{1} corresponds to the asymmetric Si-O-Si stretching vibration, confirming the presence of quartz under a well-crystallized structure.

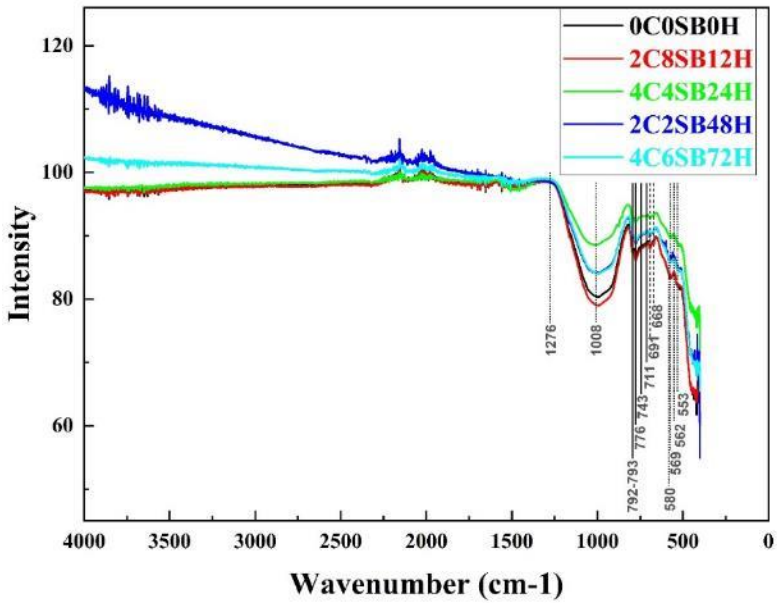

Fig. 6. FTIR analysis of mineral phases

A prominent band at 1276 cm^{-1} is likely to be due to Si-O bond deformation vibrations from secondary silicates which may point to the existence of either phyllosilicates or other silicate minerals. The bands at 668 and 691 cm^{-1} might be due to the composite of waste rock and carbonate phases of silicates, which would indicate mineral interactions. The results corroborate the hypothesis that the WCFA chemical processing gave rise to minerals mainly composed of calcite, which, in turn, improved the physical properties of the aggregate and reinforced its structure.

3.2.2 X-ray Diffraction (XRD) Analysis: Evolution of Mineral Phases After Treatment

Xray diffraction analysis showed the mineral concepts presented in the WCFA sample before and after treatment [30] (Fig. 7). The untreated sample, identified as 0C0SB0H, was predominantly made up of quartz (SiO_2) and mullite ($3Al_2O_3{\cdot}2SiO_2$) based on the results which were in agreement with earlier studies [26,57]. The presence of calcite ($CaCO_3$) that wasn't detected in the initial sample at all, was manifested in the samples 2C8SB12H and 4C4SB24H, indicating the occurrence of a chemical interaction between the cement and sodium bicarbonate in the treated samples. The calcite peaks which were additional and distinct appeared in the case of sample 2C2SB48H, whereas the calcite peaks of the sample 4C6SB72H were a lot in number and showed the highest peaks among the others thus indicating that the calcite phase had a higher rate of the formation due to the long period of immersion. The important function of immersion duration in calcium carbonate deposition has been revealed through these observations since it extends the interaction period between the cement and $NaHCO_3$.

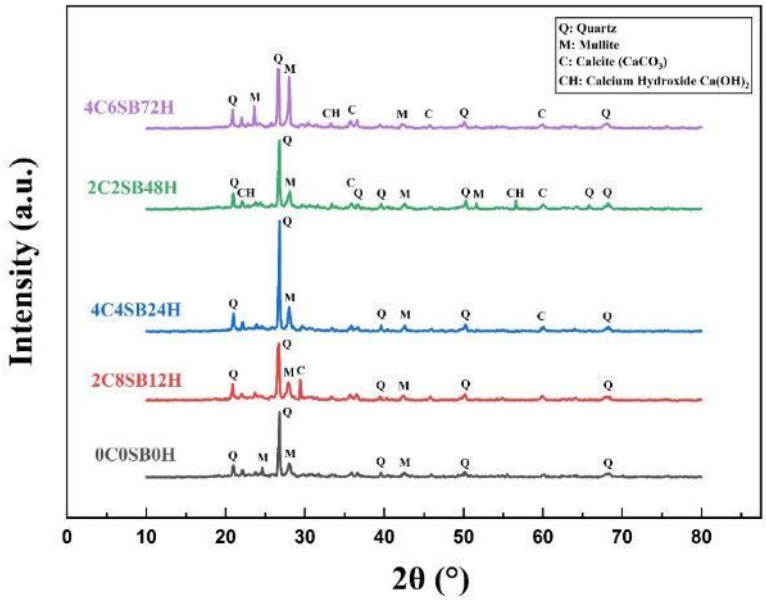

Fig. 7. X-ray diffraction analysis of mineral phase development in WCFA after chemical treatment

After treatment, calcium hydroxide (Ca $(OH)_2$) was also detected with a higher concentration for sample 2C2SB48H and sample 4C6SB72H. This shows that the initial product of cement hydration, Ca $(OH)_2$, is slowly transformed to calcium carbonate when sodium bicarbonate is present, according to Eq. (3), thus rendering calcium hydroxide an important intermediate phase in the crystallization of calcite, the ultimate product.

The quartz and mullite peak densities in all samples did not significantly change, indicating that their chemical properties were not affected by the treatment they went through. The slow evolution of calcite, promoted by the extension of time under water, reveals that the application of a mixture of cement and sodium bicarbonate results in the perfect habitat for the deposition of new carbonaceous materials, especially calcium carbonate. The observed physical improvements are due to the structural changes, which resulted in the filling of the internal voids by crystalline calcite, wherein apparent porosity and water absorption were significantly reduced, and thus, the material's density and structural strength were enhanced.

3.2.3 Morphological Analysis (SEM – Scanning Electron Microscopy) and Compositional Analysis (EDS – Energy Dispersive Spectroscopy)

The scanning electron microscopy (SEM) photographs also compare the surface morphology, while offering an insider view on the effects of chemical treatments on WCFA. The images present a substantial alteration in the porous structure and the amount of calcium carbonate ($CaCO_3$) that was precipitated influenced by the cement concentration, the sodium bicarbonate concentration, and the immersion duration. The porosity of the control sample (0C0SB0H) is quite high and the pores are quite large and open, which indicates the structure of the untreated material at the beginning (Fig. 8).

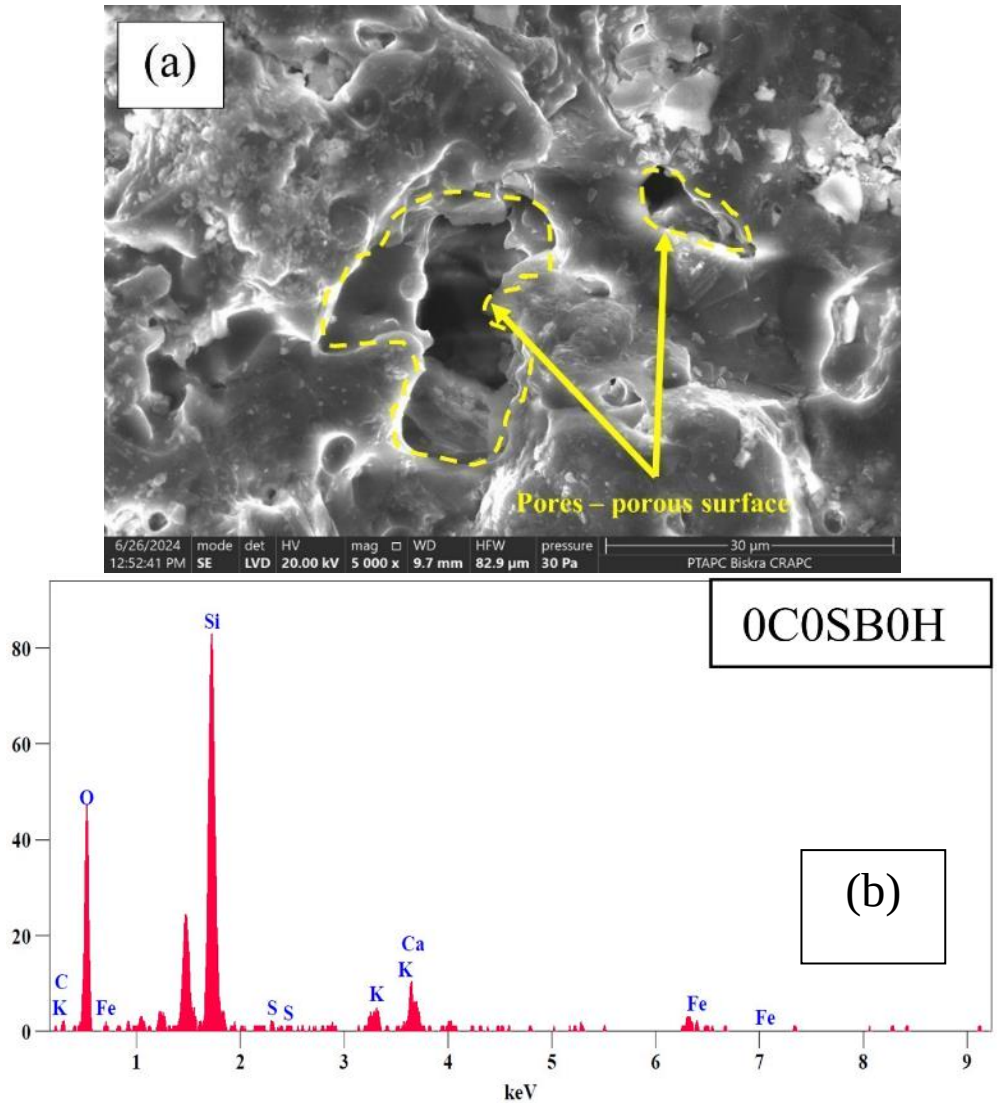

Fig. 8. Morphological analysis (a) and Compositional analysis (b) of sample 0C-0SB-0H using SEM-EDS

The analysis through energy dispersive spectroscopy (EDS) determined the composition of the samples. The control sample (0C0SB0H) did not exhibit any calcium carbonate presence and had a low calcium level (7.80%) and a negligible carbon level (4.47%) which verified the very low amounts of carbonaceous phases in the base material. On the other hand, sample 2C8SB12H experienced a dramatic reduction in open porosity, along with massive deposition of $CaCO_3$ on the grain surfaces and in the pores (Fig. 9). EDS analysis reveals a high calcium content of 9.71% (by weight) and a carbon content of 1.38 (Fig. 9), confirming the initial formation of calcium carbonate ($CaCO_3$) on the surface of the grains and in the pores. Samples 2C2SB48H and 4C6SB72H show intensified $CaCO_3$ precipitation (Fig. 10 and Fig. 11). This structural change is marked by more pore filling and densification of the aggregate surface. However, excessive packing of deposits on

4C6SB72H can be counterproductive, compromising aggregate integrity and limiting their homogeneous integration into cementitious matrices.

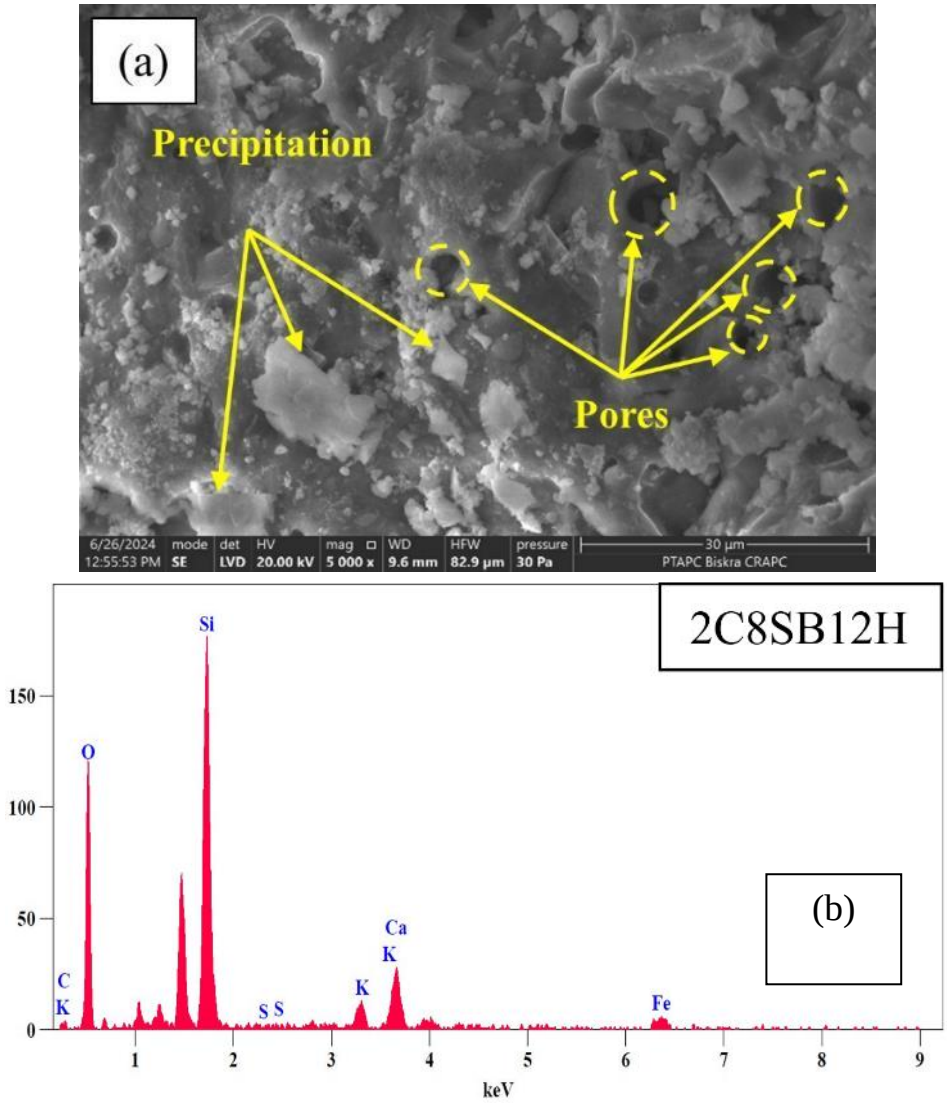

Fig. 9. Morphological (a) and elemental (b) analysis of sample 2C8SB12H by SEM -EDS

Morphological analysis (a) and Compositional analysis (b) of sample 4C6SB72H using SEM -EDS. For samples 2C2SB48H and 4C6SB72H (Fig. 10 and Fig. 11), EDS analyses reveal a significant increase in calcium (10.49% and 20.89%, respectively) and in carbon (5.31% and 20.62%).

The most promising sample, of all, is 4C4SB24H. It features a densified surface, a significantly reduced porosity and a homogeneous precipitation distribution, as revealed by the SEM observations in Fig. 12. The results of the scanning electron microscope (SEM) morphology together with the previous studies of Grabiec et al. [54], Phan et al. [73] and García-González et al. [69] , corroborate the increase in density, decrease in porosity and water absorption. They also supported the Fourier-transform infrared spectroscopy (FTIR) and X-ray diffraction (XRD) methods by uncovering the mineral phase's existence and the treatment's efficacy. For the sample 4C4SB24H (Fig. 12), the EDS analysis supports the compositional change with a consistent level of calcium (12.82%) and carbon (16.58%), thus indicating the even production of $CaCO_3$ without the extra buildup.

Energy dispersive spectroscopy (EDS) analysis results agree with the morphological observations made by scanning electron microscopy (SEM) and confirm the changes in the structure of the treated aggregate that have taken place. The calcium to carbon ratio has significantly increased which means that calcium carbonate ($CaCO_3$) is being precipitated very slowly. This statement is

supported by the substantial reduction in surface porosity and pore density which has been measured with the help of microscopic images.

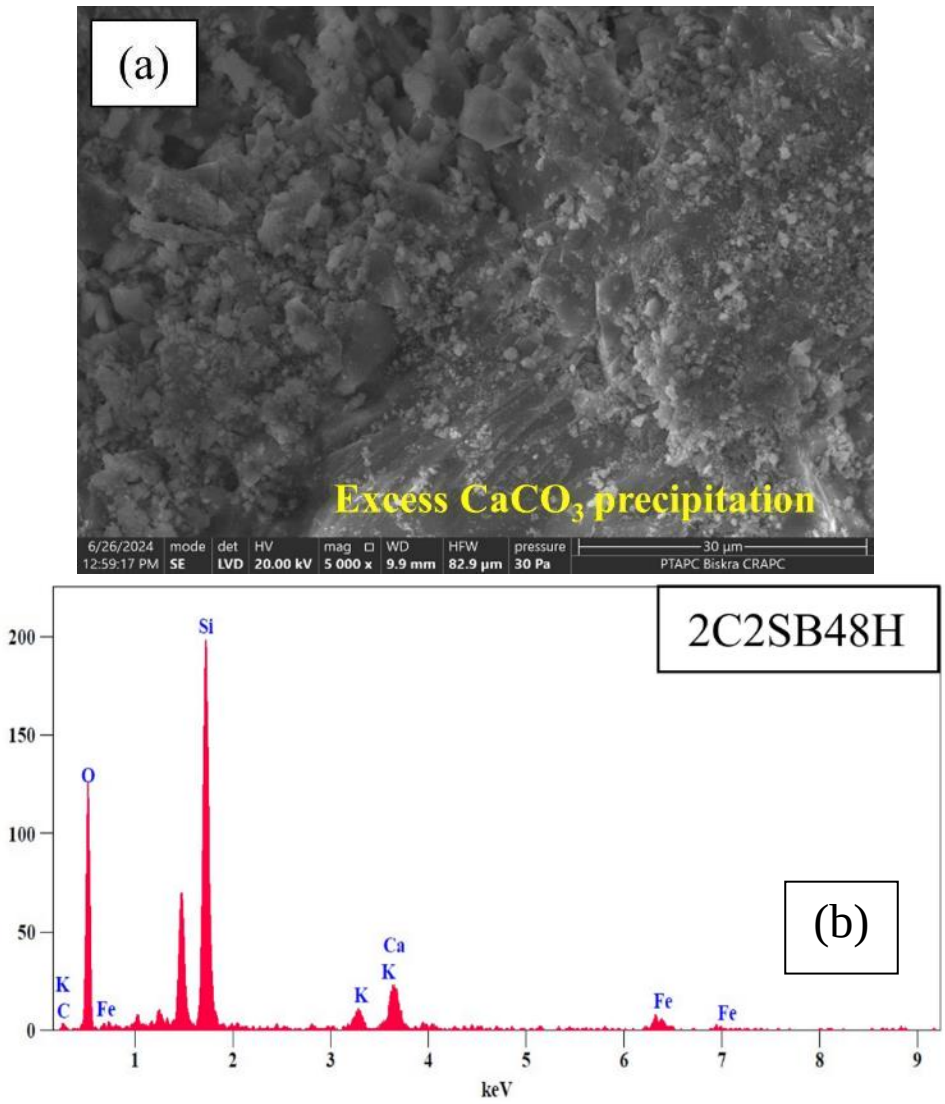

Fig. 10. Morphological analysis (a) and Compositional analysis (b) of sample 2C2SB48H using SEM -EDS.

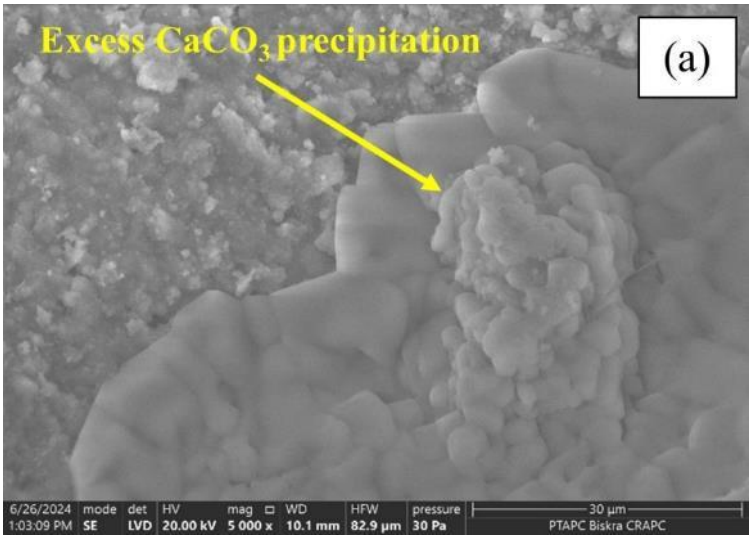

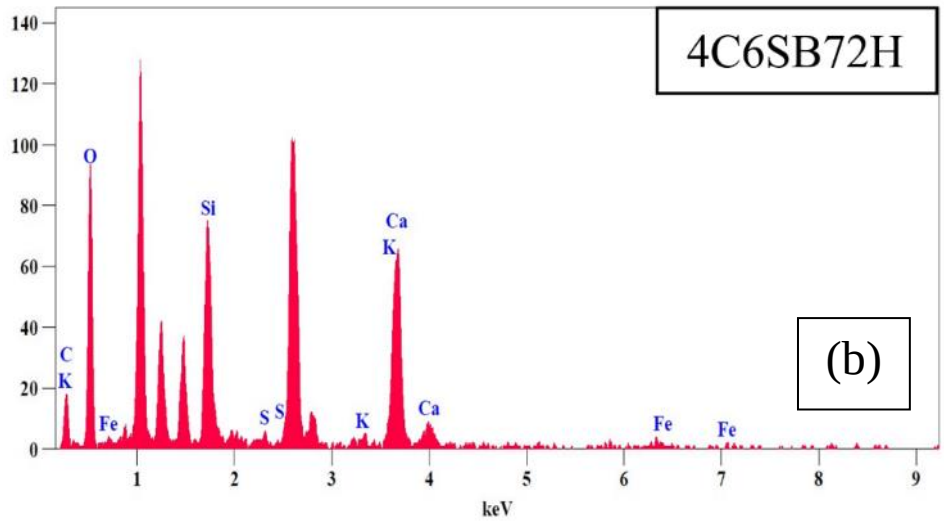

Fig. 11. Morphological analysis (a) and Compositional analysis (b) of sample 4C6SB72H using SEM -EDS

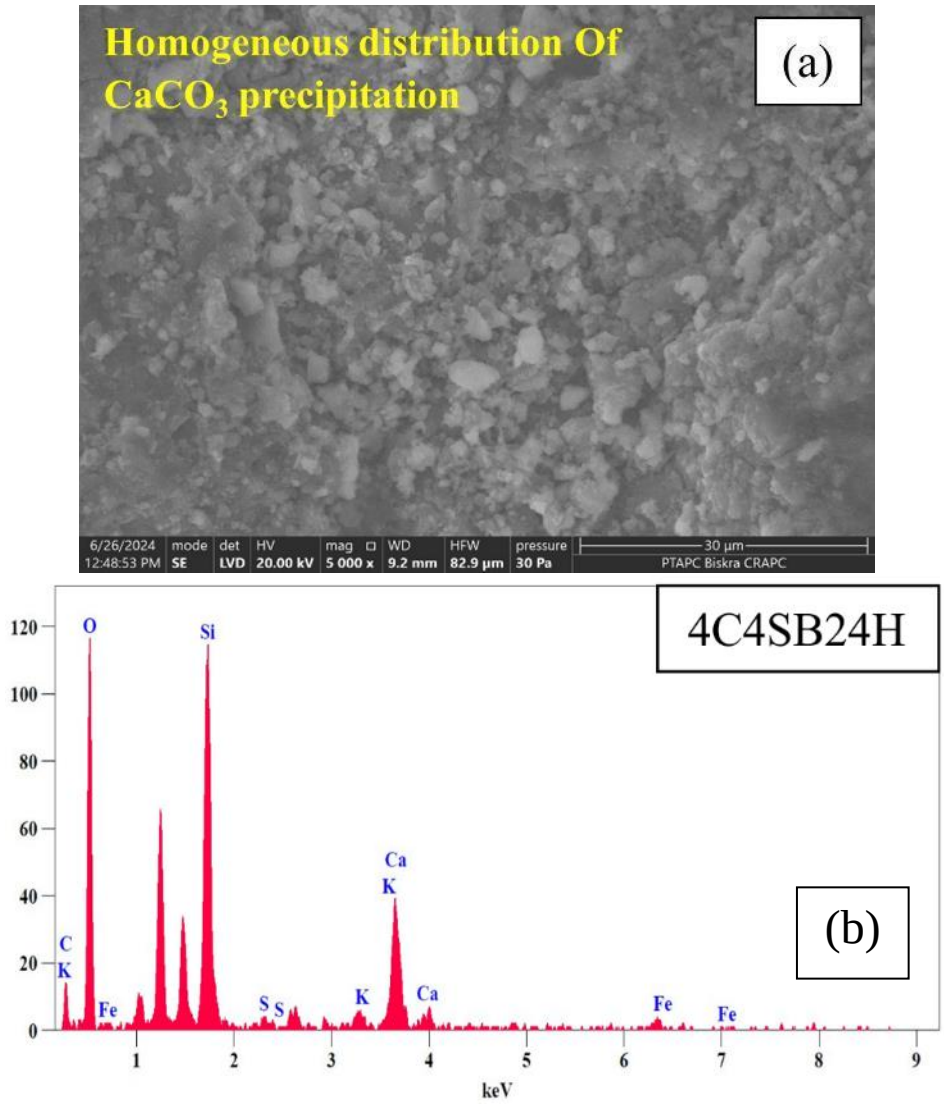

Fig. 12. Morphological analysis (a) and Compositional analysis (b) of sample 4C4SB24H using SEM -EDS

3.3 Statistical Analysis of RSM Results

Quadratic Regression analysis of data from Table 1 was performed using Design-Expert software. Relationships between response variables Y and influencing factors X1 (% C), X2 (% SB), and X3 (% H) are described by second-order regression equations [78,80,82], presented in Table 4, Table 5, and Table 6.

3.3.1 ANOVA for Quadratic Model

Table 4. Response 1 – Bulk Density

Source	Sum of Squares	df	Mean Square	F-value	p-value	
Model	0.0240	8	0.0030	52.53	< 0.0001	significant
A-Cement	0.0001	1	0.0001	2.15	0.1560	
B-Sodium Bicarbonate	0.0021	1	0.0021	36.06	< 0.0001	
C-Immersion Duration	0.0003	1	0.0003	4.47	0.0450	
AB	1.347×10^{-7}	1	1.347×10^{-7}	0.0024	0.9616	
AC	0.0011	1	0.0011	18.66	0.0002	
BC	0.0001	1	0.0001	1.41	0.2468	
B^2	0.0004	1	0.0004	7.48	0.0115	
C^2	0.0072	1	0.0072	125.54	< 0.0001	
Residual	0.0014	24	0.0001			
Cor Total	0.0253	32				

Fit Statistics			
Std. Dev.	0.0076	R^2	0.9460
Mean	1.19	Adjusted R^2	0.9280
C.V. %	0.6352	Predicted R^2	0.88646
		Adeq Precision	31.5087

$$\rho b = 1.09676 + 0.010118(A) + 0.012763(B) + 0.003542(C) + 0.000025(A \times B) - 0.000231(A \times C) - 0.000029(B \times C) - 0.000844(B^2) - 0.000039(C^2) \quad (10)$$

where, P_b = bulk density (g/cm^3), A = cement concentration (%), B = sodium bicarbonate concentration (%), C= immersion duration (hours).

Table 5. Response 2 – Absorption by Immersion

Source	Sum of Squares	df	Mean Square	F-value	p-value	
Model	6.94	8	0.8672	24.13	< 0.0001	significant
A-Cement	0.6032	1	0.6032	16.78	0.0004	
B-Sodium Bicarbonate	1.08	1	1.08	30.01	< 0.0001	
C-Immersion Duration	0.3647	1	0.3647	10.15	0.0040	
AB	0.0184	1	0.0184	0.5132	0.4807	
AC	0.2667	1	0.2667	7.42	0.0118	
BC	0.6112	1	0.6112	17.00	0.0004	
B^2	0.9026	1	0.9026	25.11	< 0.0001	
C^2	0.7119	1	0.7119	19.80	0.0002	
Residual	0.8627	24	0.0359			
Cor Total	7.80	32				

Fit Statistics			
Std. Dev.	0.1896	R^2	0.8894
Mean	4.13	Adjusted R^2	0.8525
C.V. %	4.60	Predicted R^2	0.7849
		Adeq Precision	24.1689

$$W_a = 5.95084 - 0.228902(A) - 0.498902(B) + 0.003528(C) - 0.009216(A\times B) + 0.003651(A\times C) + 0.002567(B\times C) + 0.038795(B^2) - 0.000386(C^2) \quad (11)$$

where, Wa = absorption by immersion (%), A = cement concentration (%), B = sodium bicarbonate concentration (%), C = immersion duration (hours).

Table 6. Response 3 – Apparent porosity

Source	Sum of Squares	df	Mean Square	F-value	p-value	
Model	50.68	8	6.33	35.54	< 0.0001	significant
A-Cement	0.1184	1	0.1184	0.6643	0.4231	
B-Sodium Bicarbonate	3.13	1	3.13	17.59	0.0003	
C-Immersion Duration	15.28	1	15.28	85.74	< 0.0001	
AB	0.1207	1	0.1207	0.6772	0.4186	
AC	0.0007	1	0.0007	0.0036	0.9523	
BC	2.87	1	2.87	16.12	0.0005	
B^2	5.69	1	5.69	31.93	< 0.0001	
C^2	6.84	1	6.84	38.37	< 0.0001	
Residual	4.28	24	0.1782			
Cor Total	54.95	32				

Fit Statistics			
Std. Dev.	0.4222	R^2	0.9222
Mean	9.00	Adjusted R^2	0.8962
C.V. %	4.69	Predicted R^2	0.8591
		Adeq Precision	30.1690

$$\varepsilon = 14.18613 + 0.028295(A) - 1.12784(B) - 0.151927(C) - 0.023575(A\times B) + 0.000180(A\times C) + 0.005566(B\times C) + 0.097417(B^2) + 0.001196(C^2) \quad (12)$$

where ε = apparent porosity (%), A = cement concentration (%), B = sodium bicarbonate concentration (%), C = immersion duration (hours).

3.3.2 ANOVA and Interaction Analysis

Analysis of variance shows R^2 values for bulk density, water absorption, and apparent porosity of 0.9460, 0.8894, and 0.9222 respectively, reflecting a strong correlation between predicted and actual values. This confirms that the regression model has a good fit with different tests on the data [79,81,87]. Moreover, the corresponding adjusted R^2 values were found to be 0.9280, 0.8525, and 0.8962 for *ρb*, *Wa*, and *ε* apparent porosity in that order. Thus, the quadratic model clarifies the variance in the response variables up to 92.80%, 85.25%, and 89.62% respectively, with only 7.20%, 14.75%, and 10.38% of the total variance remaining unexplained. Fig. 13 shows the correlation between the predicted and actual values, which closely align with a straight line, indicating a strong fit between the experimental and predicted data. Fig. 14 shows the normal distribution of residuals. An alignment of points along a straight line indicates that the errors follow a normal distribution and that no variance deviation is observed for all responses. In Fig. 15, the residuals are plotted against the predicted values. The random dispersion of the points indicates

that the assumptions of independence of errors and constant variance are satisfied for all response variables.

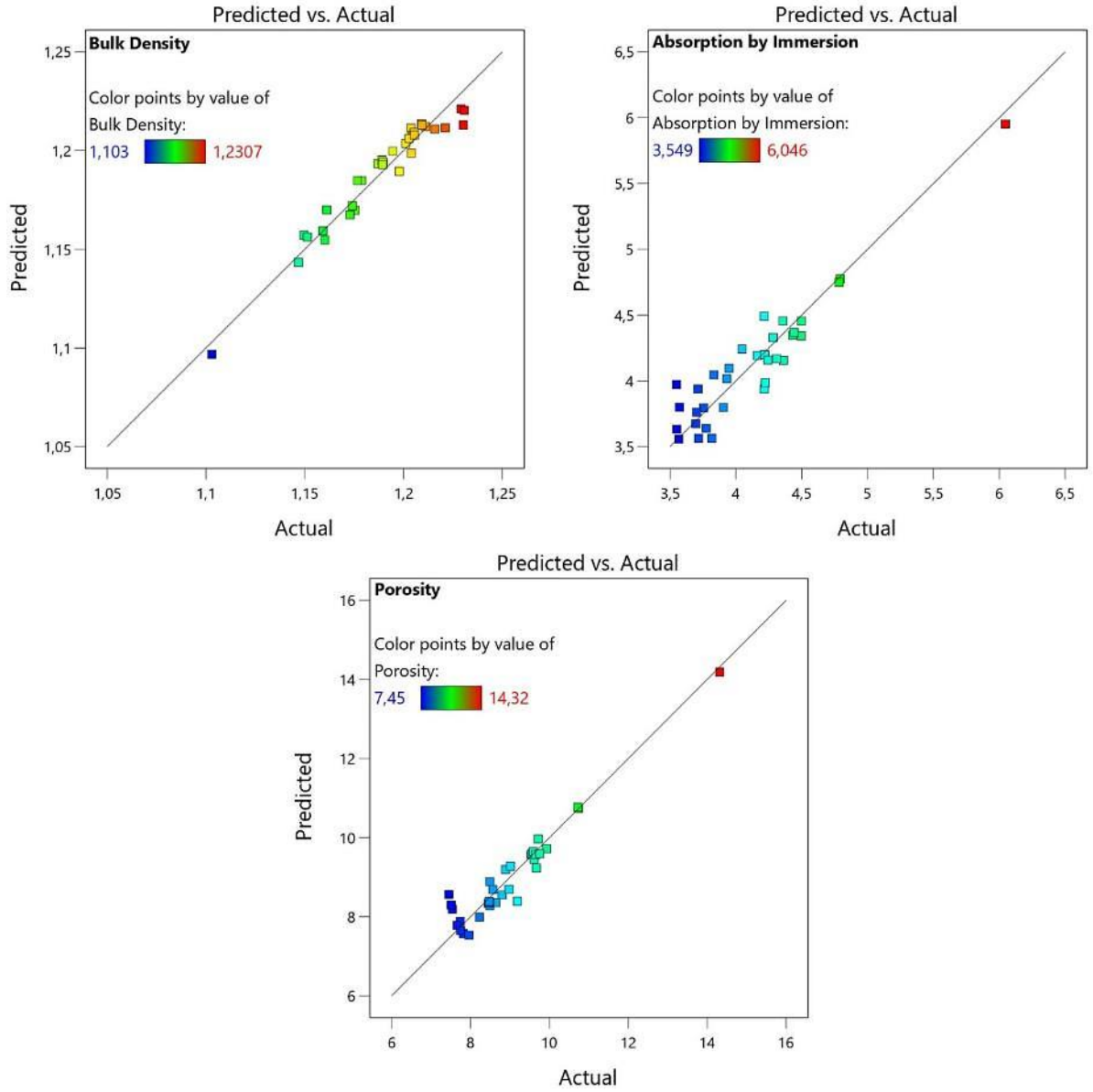

Fig. 13. Relationship between predicted and actual values for WCFA

All the above results confirm that the presented regression equations are adapted to the prediction of bulk density, water absorption and apparent porosity. In addition, the model works effectively to optimize the preparation parameters of WCFA treated with C and SB solution.

The data shown in Table 4, Table 5, and Table 6 for the analysis of variance (ANOVA) confirm the correctness as well as the dependability of the regression models that were developed for the purpose of predicting the bulk density, water absorption, and apparent porosity of WCFA. The bulk density model produced an F value of 52.53 which means a very high significance level ($p < 0.01\%$). The factors B, C, AC, B^2, and C^2 are the most influential ones on the response. In the same way, the water absorption model was also very significantly validated through the statistical test ($F = 24.13$; $p < 0.01$), where the coefficients A, B, C, AC, BC, B^2, and C^2 had the most pronounced impacts. The apparent porosity model at the same time indicated a very high statistical significance as well ($F = 35.54$; $p < 0.01$), with the factors being B, C, BC, B^2, and C^2.

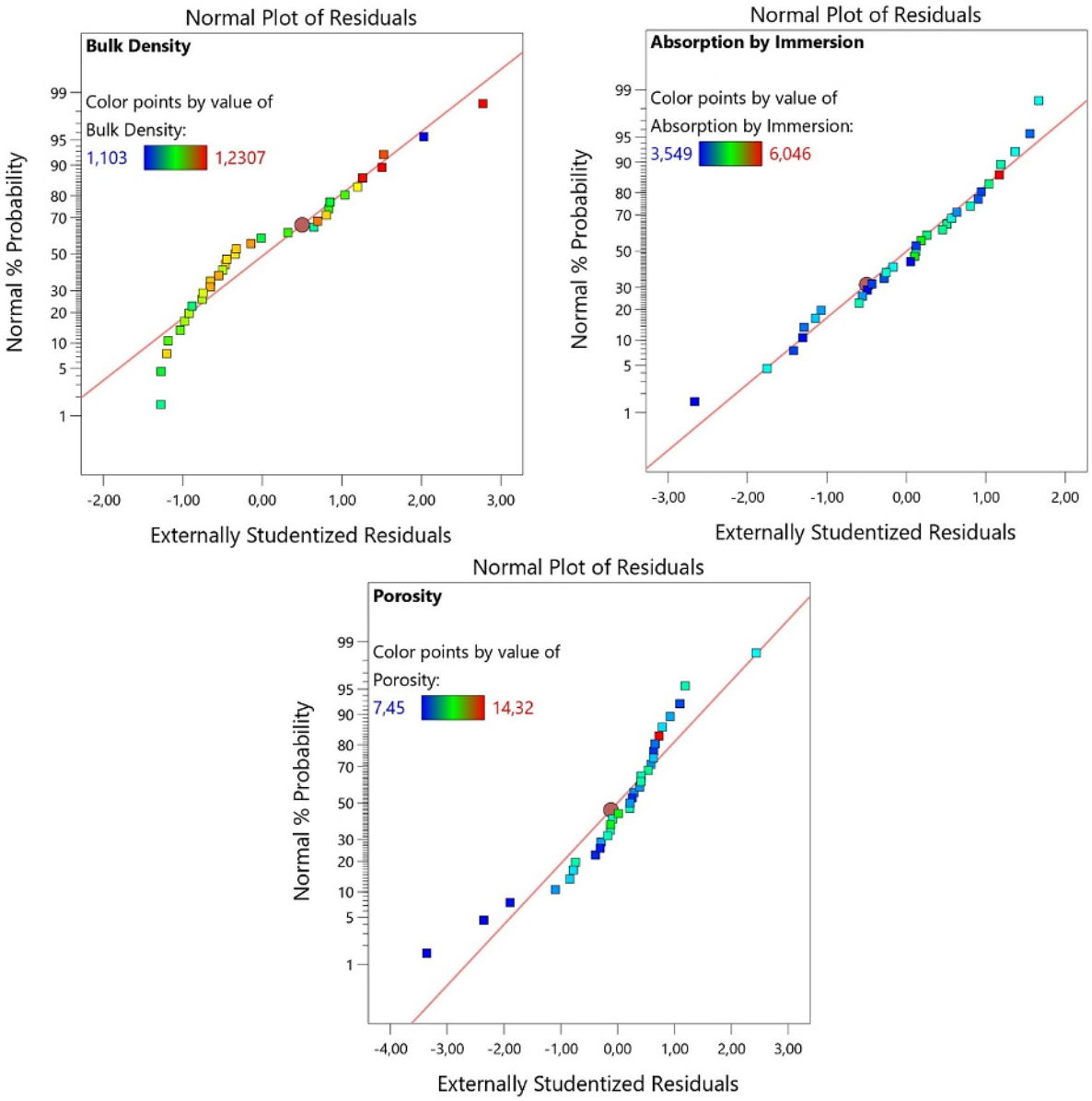

Fig. 14. Normal probability plots of residuals for WCFA

The proposed models are characterized by good predictive accuracy as evidenced by the predicted R^2 values of 0.8646 for bulk density, 0.7849 for water absorption, and 0.8591 for apparent porosity. So, the empirical Eqs. (10)-(11)-(12) can represent the link between treatment parameters and physical properties, hence allowing WCFA treatment to be optimized systematically and efficiently for its application in sustainable construction to the fullest.

The conformity of the second-order polynomial regression models developed for bulk density, water absorption, and apparent porosity to variance analysis (ANOVA) was demonstrated, with excellent statistical performance displayed by all the models. The predicted R^2 and adjusted R^2 of each model are closely interconnected as their greatest disparity does not go beyond 0.2 (0.8646 vs. 0.9280; 0.7849 vs. 0.8525; 0.8591 vs. 0.8962) which is a strong confirmation of the models' validity and high predictive power without any overfitting.

The values of adequate precision, which serve as an indication of the signal-to-noise ratio, were significantly higher than the recommended minimum (4) [88,89], and were found to be 31.509, 24.169, and 30.169 for bulk density, water absorption, and apparent porosity, respectively. This refers to a very strong and reliable signal while allowing the model fully and faithfully to explore the entire space of the experiment.

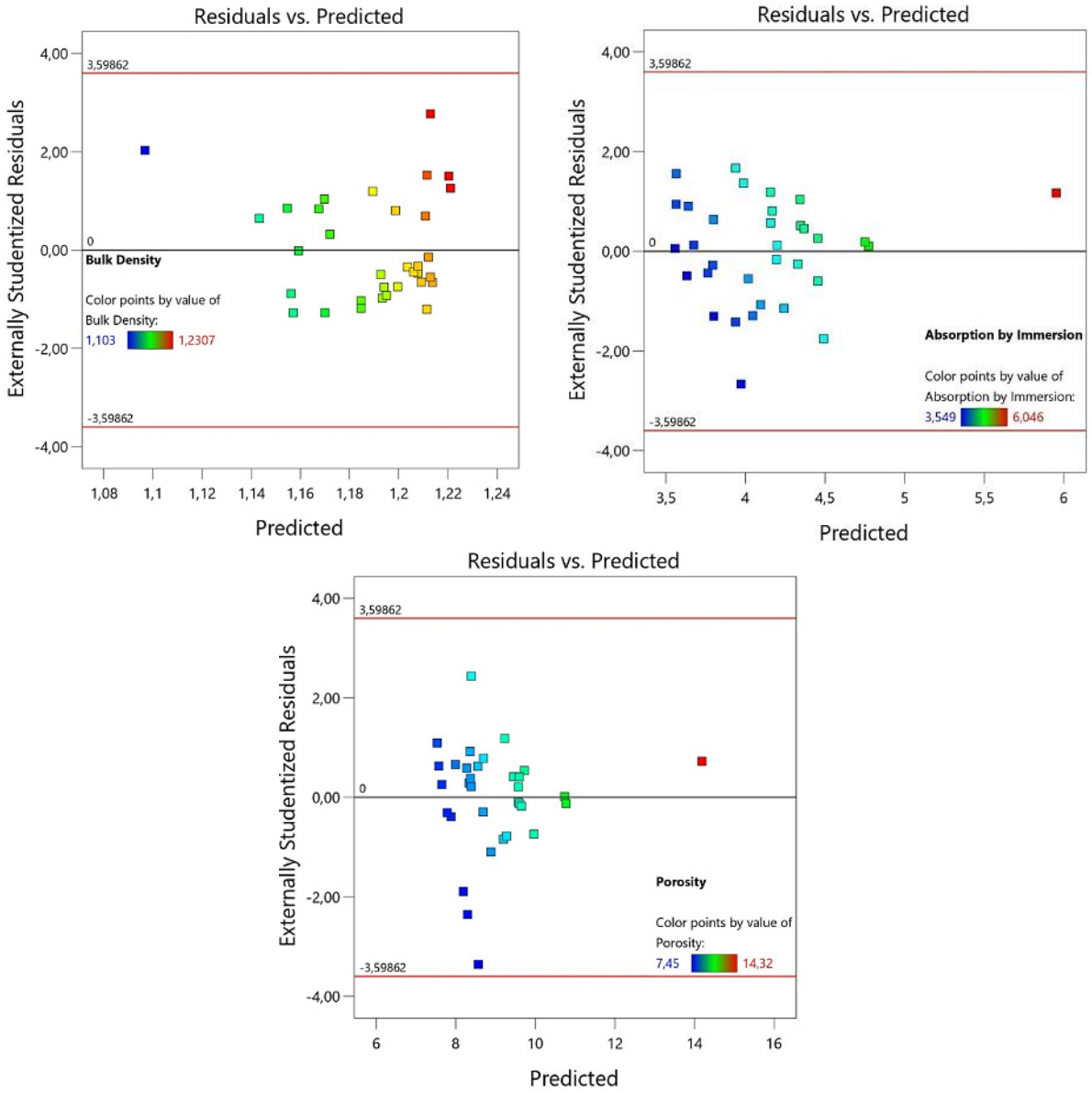

Fig. 15. Residuals vs. Predicted values for bulk density, water absorption, and apparent porosity of WCFA

Consequently, the studied response variables and the best conditions for WCFA treatment were predicted accurately by second-degree polynomial equations which were derived from the Box-Behnken experimental design. The models' accuracy and statistical validity are presented through Fig. 13, Fig. 14, and Fig. 15which all exhibit a random distribution of residuals devoid of any systematic pattern, thus confirming the models' accuracy and statistical validity. These results highlight the models' ability to accurately unravel the complex interrelation between process variables and, on the other hand, to allow the structured optimization of the WCFA performance in sustainable construction applications.

The surfaces of responses along with the curves of contours (Fig. 16 and Fig. 17) clearly show how the factors of C, SB, and H interrelate and the physical properties of the treated aggregates that result. The experiments conducted evidently indicate that, through prolonged immersion, substantial and consistent enhancement of performance is achieved by the simultaneous raising of both cement and sodium bicarbonate concentrations, these factors result in increased bulk density, reduced water absorption, and decreased apparent porosity.

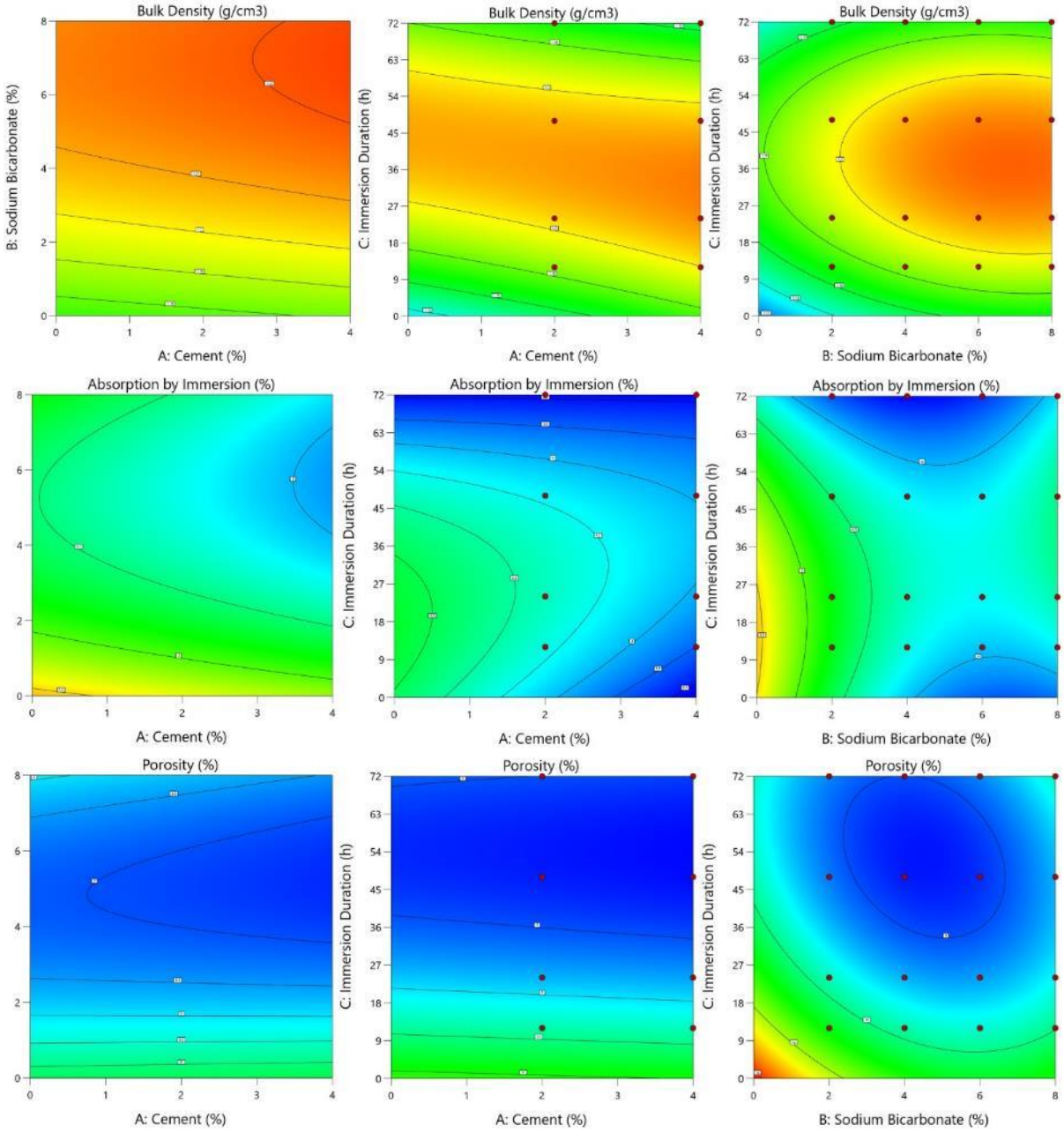

Fig. 16. 2D contour curves representing bulk density, water absorption and apparent porosity as a function of (C/SB), (C/ID), and (SB/ID) interactions for treated WCFA

After analyzing the influence of experimental parameters on bulk density, water absorption and apparent porosity of WCFA treated with cement (C) and sodium bicarbonate (SB), the ranges of these variables and the optimization approach (goal and importance) leading to the optimum values are presented in Table 7. The models were optimized using the desirability function of Design-Expert software. This functionality enables determining of the best input and output parameters (target responses) at the same time according to the given input conditions, as depicted in Fig. 18. The model forecasts optimal values like 1.213 g/cm^3 for bulk density, 3.972% for water absorption, and 8.564% for apparent porosity. The mentioned results correlate to the optimal experimental conditions of 4% cement, 4% sodium bicarbonate and 24 hours of immersion, which are presented in Table 8.

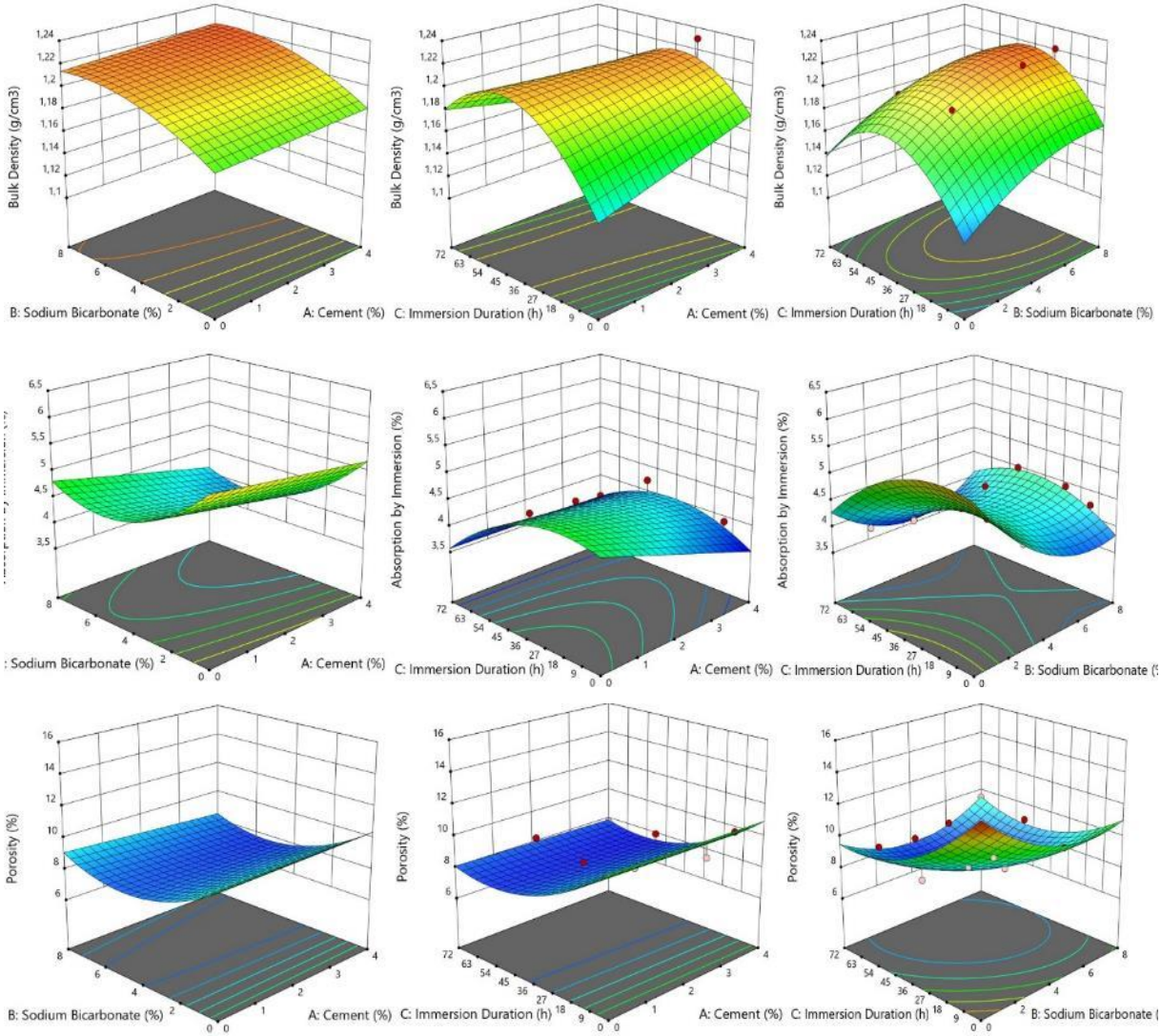

Fig. 17. 3D response graphs RSM models for bulk density, water absorption, and apparent porosity as a function of (C/SB), (C/ID), and (SB/ID) interactions of treated WCFA

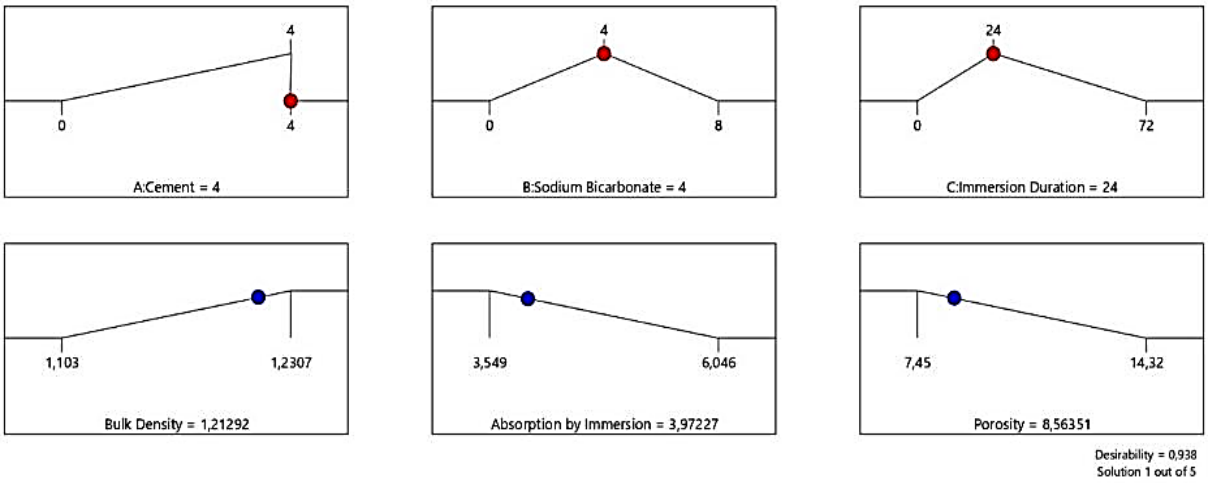

Fig. 18. Desirability ramps for optimum values for ρb, Wa, and ε of processed WCFA

Table 7. Treated WCFA stress factors and their responses

Name	Goal	Lower Limit	Upper Limit	Importance
A: Cement (%)	is target = 4	0	4	5
B: Sodium Bicarbonate (%)	is target = 4	0	8	5
C: Immersion Duration (hours)	is target = 24	0	72	5
Bulk Density (g/cm^3)	maximize	1.103	1.2307	3
Absorption by Immersion (%)	minimize	3.549	6.046	3
Apparent porosity (%)	minimize	7.45	14.32	3

Table 8. The five best solutions for WCFA treatment parameters and their corresponding responses

Number	Cement (%)	Sodium Bicarbonate (%)	Immersion Duration (hours)	Bulk Density (g/cm^3)	Absorption by Immersion (%)	Apparent porosity (%)	Coefficient of Desirability	
1	4.000	4.000	24.000	1.213	3.972	8.564	0.938	Selected
2	4.000	4.000	24.288	1.213	3.975	8.543	0.937	
3	4.000	4.000	24.580	1.213	3.978	8.522	0.936	
4	4.000	4.000	25.181	1.214	3.983	8.481	0.935	
5	4.000	4.000	21.388	1.211	3.944	8.758	0.911	

4. Conclusion

This study explored the impact of using a suspension of cement and sodium bicarbonate on the properties of recycled fine aggregate from ceramic waste (WCFA). The main results are as follows:

- Treatment of WCFA with the cement and sodium bicarbonate combination improved bulk density, apparent porosity and water absorption by immersion of all treated samples.
- The highest performance was shown by the sample treated with a solution containing 4% cement, 4% $NaHCO_3$, and 24 hours of immersion, which showed an 11.5% increase in density, a 41.3% decrease in water absorption, and a 47.9% reduction in apparent porosity compared to the untreated sample.
- FTIR and XRD techniques provided the evidence for the presence of calcium carbonate ($CaCO_3$) in the treated aggregates, which helped to lessen the porosity.
- The results of SEM imaging also supported the fact that there was a considerable improvement in the structure of WCFA due to chemical treatment, which was marked by the pores being filled with calcium carbonate ($CaCO_3$) precipitates.
- It has been observed that increasing the concentration of cement and sodium bicarbonate, as well as extending the immersion duration, generally improves the physical properties of fine ceramic aggregates (WCFA). But excessive immersion duration causes over-precipitation of calcium carbonate ($CaCO_3$), which may impair the internal cohesion of the aggregates with no significant physical property improvement.
- The output of the statistical models through analysis of variance (ANOVA) revealed the physical properties of the treated ceramic aggregates to be statistically significant at a very high level, with an error rate lower than 7%.
- It was found that the best physical performance could be achieved in treating fine ceramic particles with 4% cement and sodium bicarbonate each for 24 h of immersion. Using these optimal ratios, the modified model predicted a density of 1.213 g/cm^3, a water absorption by immersion of 3.972%, and an apparent porosity of 8.564%. These predictive results were confirmed by experimental results, with the aim of attesting to the reliability of the optimized model developed by RSM.

In order to carry on with this research, we propose the addition of the treated WCFA at its best conditions (C: 4%, SB:4%, and ID: 24 hours) into a cement mix with the sand of dunes. Their impact on the mechanical properties, durability, and microstructure of ecological mortars will be studied for the purpose of discovering the best and the most sustainable formulation.

Nomenclature

WCFA	Waste Ceramic Fine Aggregates.	C_3S	tricalcium silicate.
C	Cement content (%).	H_2O	Water.
SB	Sodium bicarbonate (%).	CSH	Calcium silicate hydrate
ID	Immersion Duration (h).	Na_2CO_3	Sodium carbonate.
XRD	X-ray diffraction.	Cu	Coefficient of Uniformity.
FTIR	Fourier Transform Infrared Spectroscopy.	Cc	Coefficient of Curvature.
SEM:	Scanning Electron Microscopy.	ρ_a	Bulk Density (g/cm^3).
EDS	Energy Dispersive Spectroscopy.	ρ_s	Absolute Density (g/cm^3).
BBD	Box-Behnken Design	ε	Apparent Porosity (%).
RSM	Response Surface Model	Wa	water absorption by immersion (%).
CDW	Construction and Demolition Waste	SSD	Saturated Surface Dry.
RCA	Recycled Concrete Aggregates.	ASTM	American Society for Testing and Materials
HCl	Hydrochloric acid	EN	European standard
$C_2H_4O_2$	Acetic acid.	ANOVA	Analysis of Variance.
CaCO3	Calcium carbonate.	R^2	Coefficient of determination.
NaHCO3	Sodium bicarbonate.	F	F-value in ANOVA.
C_2S	dicalcium silicate.	P	P-value in ANOVA.
$Ca(OH)_2$	Calcium hydroxide.		

(i=0,2,4)C(j=0,2,4)SB(k=0,12,24,48,75)H Sample code used to denote treatment conditions

Acknowledgements

The authors warmly thank the Directorate General for Scientific Research and Technological Development (DGRSDT) for their support in this work. As well as all the persons in charge of the Unit for the development of renewable energy in arid areas (UDERZA). Without forgetting the Laboratory of exploitation and valorization of Saharan energy resources (LEVRE), faculty of exact sciences, University of El Oued.

References

[1] Alanyali H, Çöl M, Yilmaz M, Karagöz Ş. Concrete produced by steel-making slag (basic oxygen furnace) addition in portland cement. Int J Appl Ceram Technol 2009;6:736–48. https://doi.org/10.1111/j.1744-7402.2008.02317.x.
[2] Hebhoub H, Aoun H, Belachia M, Houari H, Ghorbel E. Use of waste marble aggregates in concrete. Constr Build Mater 2011;25:1167–71. https://doi.org/10.1016/j.conbuildmat.2010.09.037.
[3] Comisión Permanente del Hormigón. Code on Structural Concrete (EHE-08). Madrid: Ministerio de Fomento; 2010.
[4] British Standards Institution. Concrete – Complementary British Standard to BS EN 206. London: BSI; 2016.
[5] Works Bureau Technical Circular No. 12/2002. Hong Kong: Works Bureau; 2002.
[6] DIN 4226-100. Aggregates for mortar and concrete – Part 100: Recycled aggregates. Berlin: Deutsches Institut für Normung; 2002.
[7] NEN-EN 12620+A1. Aggregates for concrete. Delft: Nederlands Normalisatie-instituut; 2008.
[8] Li L, Liu Z, Liu W, Wang Z, Zhou C, Zeng Q. Microstructure and transport properties of cement mortar made with recycled fine ceramic aggregates. Dev Built Environ 2025;22:100643. https://doi.org/10.1016/j.dibe.2025.100643.
[9] Silva J, De Brito J, Veiga R. Partial replacement of cement with fine ceramics in rendering mortars. Mater Struct 2008;41:1333–44. https://doi.org/10.1617/s11527-007-9332-z.

[10] Frías M, Rodríguez O, Vegas I, Vigil R. Properties of calcined clay waste and its influence on blended cement behavior. J Am Ceram Soc 2008;91:1226–30. https://doi.org/10.1111/j.1551-2916.2008.02289.x.
[11] Sánchez De Rojas MI, Marín FP, Frías M, Rivera J. Properties and performances of concrete tiles containing waste fired clay materials. J Am Ceram Soc 2007;90:3559–65. https://doi.org/10.1111/j.1551-2916.2007.01944.x.
[12] Sánchez De Rojas MI, Marín F, Rivera J, Frías M. Morphology and properties in blended cements with ceramic wastes as a pozzolanic material. J Am Ceram Soc 2006;89:3701–5. https://doi.org/10.1111/j.1551-2916.2006.01279.x.
[13] Sánchez De Rojas MI, Frías M, Rivera J, Escorihuela MJ, Marín FP. Research on the pozzolanic activity of waste materials from calcined clay. Mater Constr 2001;51:45–52. https://doi.org/10.3989/mc.2001.v51.i261.379.
[14] Puertas F, García-Díaz I, Barba A, Gazulla MF, Palacios M, Gómez MP, et al. Ceramic wastes as alternative raw materials for Portland cement clinker production. Cem Concr Compos 2008;30:798–805. https://doi.org/10.1016/j.cemconcomp.2008.06.003.
[15] Binici H. Effect of crushed ceramic and basaltic pumice as fine aggregates on concrete mortars properties. Constr Build Mater 2007;21:1191–7. https://doi.org/10.1016/j.conbuildmat.2006.06.002.
[16] Pereira J, Brito J, Correia JR. Effects on concrete durability of using recycled ceramic aggregates. Mater Struct 2005;38:157–64. https://doi.org/10.1617/s11527-005-9014-7.
[17] Brito J, Pereira AS, Correia JR. Mechanical behaviour of non-structural concrete made with recycled ceramic aggregates. Cem Concr Compos 2005;27:429–33. https://doi.org/10.1016/j.cemconcomp.2004.07.005.
[18] Debieb F, Kenai S. The use of coarse and fine crushed bricks as aggregate in concrete. Constr Build Mater 2008;22:886–93. https://doi.org/10.1016/j.conbuildmat.2006.12.013.
[19] De Brito J. Structural concrete with incorporation of coarse recycled concrete and ceramic aggregates: Durability performance. Mater Struct 2009;42:663–75. https://doi.org/10.1617/s11527-008-9411-9.
[20] Guerra I, Vivar I, Llamas B, Juan A, Moran J. Eco-efficient concretes: The effects of using recycled ceramic material from sanitary installations on the mechanical properties of concrete. Waste Manag 2009;29:643–6. https://doi.org/10.1016/j.wasman.2008.06.018.
[21] Juan-Valdés A, Llamas B, Morán J. Re-use of construction and demolition residues and industrial wastes for the elaboration of recycled eco-efficient concretes. Span J Agric Res 2010;8:34–44. https://doi.org/10.5424/sjar/2010081-1140.
[22] Koyuncu H, Guney Y, Yilmaz G, Koyuncu S, Bakis R. Utilization of ceramic wastes in the construction sector. Key Eng Mater 2004;264–268:2509–12. https://doi.org/10.4028/www.scientific.net/KEM.264-268.2509.
[23] Torkittikul P, Chaipanich A. Utilization of ceramic waste as fine aggregate within Portland cement and fly ash concretes. Cem Concr Compos 2010;32:440–9. https://doi.org/10.1016/j.cemconcomp.2010.02.004.
[24] Andreola F, Barbieri L, Lancellotti I, Leonelli C. Recycling of industrial wastes in ceramic manufacturing: State of the art and glass case studies. Ceram Int 2016;42:13333–8. https://doi.org/10.1016/j.ceramint.2016.05.205.
[25] Siddesha H. Experimental studies on the effect of ceramic fine aggregate on the strength properties of concrete. Int J Eng Sci Technol 2011;3:71–6.
[26] Tabak Y, Kara M, Günay E, Yildirim ST, Yilmaz Ş. Ceramic tile waste as a waste management solution for concrete. In: Proceedings of the 3rd International Conference on Industrial and Hazardous Waste Management; September 2012; Chania, Greece. 2012. p. 1–8.
[27] Coelho A, De Brito J. Economic viability analysis of a construction and demolition waste recycling plant in Portugal – Part I: Location, materials, technology and economic analysis. J Clean Prod 2013;39:338–52. https://doi.org/10.1016/j.jclepro.2012.08.024.
[28] Khatib JM. Properties of concrete incorporating fine recycled aggregate. Cem Concr Res 2005;35:763–9. https://doi.org/10.1016/j.cemconres.2004.06.017.
[29] Djedid T, Mani M, Ouakouak A, Guettala A. Effect of varying silica-limestone sand fines on the physical-mechanical performance of concrete. Frattura ed Integrità Strutturale 2022;16:580–91. https://doi.org/10.3221/IGF-ESIS.59.38.
[30] Djedid T, Mani M, Guettala A, Hima A. Analysis of workability, mechanical strength and durability by the FT-IR method of concrete based on silica-limestone sand preserved in aggressive environments. Frattura ed Integrità Strutturale 2021;15:566–79. https://doi.org/10.3221/IGF-ESIS.59.37.
[31] Agrela F, Sánchez De Juan M, Ayuso J, Geraldes VL, Jiménez JR. Limiting properties in the characterisation of mixed recycled aggregates for use in the manufacture of concrete. Constr Build Mater 2011;25:3950–5. https://doi.org/10.1016/j.conbuildmat.2011.04.027.

[32] Evangelista L, De Brito J. Durability performance of concrete made with fine recycled concrete aggregates. Cem Concr Compos 2010;32:9–14. https://doi.org/10.1016/j.cemconcomp.2009.09.005.
[33] Medina C, Sánchez De Rojas MI, Frías M. Freeze-thaw durability of recycled concrete containing ceramic aggregate. J Clean Prod 2013;40:151–60. https://doi.org/10.1016/j.jclepro.2012.08.042.
[34] Richardson A, Coventry K, Bacon J. Freeze/thaw durability of concrete with recycled demolition aggregate compared to virgin aggregate concrete. J Clean Prod 2011;19:272–7. https://doi.org/10.1016/j.jclepro.2010.09.014.
[35] Rodrigues F, Evangelista L, De Brito J. Physical, chemical and mineralogical characterization of fine aggregates from construction and demolition waste recycling plants. J Clean Prod 2013;52:438–45. https://doi.org/10.1016/j.jclepro.2013.02.023.
[36] De Brito J. Influence of the pre-saturation of recycled coarse concrete aggregates on concrete properties. Mag Concr Res 2011;63:617–27. https://doi.org/10.1680/macr.2011.63.8.617.
[37] Wattanasiriwech D, Saiton A, Wattanasiriwech S. Paving blocks from ceramic tile production waste. J Clean Prod 2010;17:1663–8. https://doi.org/10.1016/j.jclepro.2009.08.008.
[38] Kou SC, Poon CS, Agrela F. Comparisons of natural and recycled aggregate concretes prepared with the addition of different mineral admixtures. Cem Concr Compos 2011;33:788–95. https://doi.org/10.1016/j.cemconcomp.2011.05.009.
[39] Halicka A, Ogrodnik P, Zegardlo B. Using ceramic sanitary ware waste as concrete aggregate. Constr Build Mater 2013;48:295–305. https://doi.org/10.1016/j.conbuildmat.2013.06.063.
[40] Medina C, Sánchez De Rojas MI, Frías M. Reuse of sanitary ceramic wastes as coarse aggregate in eco-efficient concretes. Cem Concr Compos 2012;34:48–54. https://doi.org/10.1016/j.cemconcomp.2011.08.015.
[41] Profile SEE. The use of waste ceramic tile in cement production. Cem Concr Res 2000;30:0–3. https://doi.org/10.1016/S0008-8846(00)00202-7.
[42] Anderson DJ, Smith ST, Au FTK. Mechanical properties of concrete utilising waste ceramic as coarse aggregate. Constr Build Mater 2016;117:20–8. https://doi.org/10.1016/j.conbuildmat.2016.04.153.
[43] Alves AV, Vieira TF, De Brito J, Correia JR. Mechanical properties of structural concrete with fine recycled ceramic aggregates. Constr Build Mater 2014;64:103–13. https://doi.org/10.1016/j.conbuildmat.2014.04.037.
[44] Medina C, Frías M, Sánchez De Rojas MI, Thomas C, Polanco JA. Gas permeability in concrete containing recycled ceramic sanitary ware aggregate. Constr Build Mater 2012;37:597–605. https://doi.org/10.1016/j.conbuildmat.2012.08.023.
[45] Pereira-de-Oliveira LA, Castro-Gomes JP, Santos PMS. The potential pozzolanic activity of glass and red-clay ceramic waste as cement mortars components. Constr Build Mater 2012;31:197–203. https://doi.org/10.1016/j.conbuildmat.2011.12.110.
[46] O'Farrell M, Sabir BB, Wild S. Strength and chemical resistance of mortars containing brick manufacturing clays subjected to different treatments. Cem Concr Compos 2006;28:790–9. https://doi.org/10.1016/j.cemconcomp.2006.05.014.
[47] Silva J, De Brito J, Veiga R. Incorporation of fine ceramics in mortars. Constr Build Mater 2009;23:556–64. https://doi.org/10.1016/j.conbuildmat.2007.10.014.
[48] Barbudo A, De Brito J, Evangelista L, Bravo M, Agrela F. Influence of water-reducing admixtures on the mechanical performance of recycled concrete. J Clean Prod 2013;59:93–8. https://doi.org/10.1016/j.jclepro.2013.06.022.
[49] Matias D, De Brito J, Rosa A, Pedro D. Mechanical properties of concrete produced with recycled coarse aggregates – Influence of the use of superplasticizers. Constr Build Mater 2013;44:101–9. https://doi.org/10.1016/j.conbuildmat.2013.03.011.
[50] Brown T, Taylor AH. Performance of concrete made with commercially produced coarse recycled concrete aggregate. Cem Concr Res 2001;31:0–0.
[51] Juan-Valdés A, Pozo J, Guerra-Romero MI. Pre-saturation technique of recycled aggregates: solution to the water absorption drawback in recycled concrete manufacture. Materials (Basel) 2014;7:6224–42. https://doi.org/10.3390/ma7096224.
[52] Ismail S, Ramli M. Mechanical strength and drying shrinkage properties of concrete containing treated coarse recycled concrete aggregates. Constr Build Mater 2014;68:726–39. https://doi.org/10.1016/j.conbuildmat.2014.06.058.
[53] Spaeth V, Tegguer AD. Improvement of recycled concrete aggregate properties by polymer treatments. Int J Sustain Built Environ 2014;2:143–52. https://doi.org/10.1016/j.ijsbe.2014.03.003.
[54] Grabiec AM, Klama J, Zawal D, Krupa D. Modification of recycled concrete aggregate by calcium carbonate biodeposition. Constr Build Mater 2012;34:145–50. https://doi.org/10.1016/j.conbuildmat.2012.02.027.

[55] Mukherjee A, Basu PC, Reddy MS. Lactose mother liquor as an alternative nutrient source for microbial concrete production by Sporosarcina pasteurii. J Ind Microbiol Biotechnol 2009;36:433–8. https://doi.org/10.1007/s10295-008-0514-7.
[56] Chunxiang Q, Jianyun W, Ruixing W, Liang C. Corrosion protection of cement-based building materials by surface deposition of $CaCO_3$ by Bacillus pasteurii. Mater Sci Eng C 2009;29:1273–80. https://doi.org/10.1016/j.msec.2008.10.025.
[57] Shah KW, Huseien GF. Recycled ceramics in sustainable concrete: properties and performance. 1st ed. Boca Raton (FL): CRC Press; 2021.
[58] Yacine A, Ratiba M, Abderrahmane G. Ceramic waste influence on dune sand mortar performance. Constr Build Mater 2016;125:703–13. https://doi.org/10.1016/j.conbuildmat.2016.08.083.
[59] Senthamarai RM, Manoharan PD. Concrete with ceramic waste aggregate. Cem Concr Compos 2005;27:910–3. https://doi.org/10.1016/j.cemconcomp.2005.04.003.
[60] Wang J, Zhang R, Hou F, Ye G. Influence of pore property and alkalinity on the bio-deposition treatment efficiency of recycled aggregates. J Build Eng 2025;89:109381. https://doi.org/10.1016/j.jobe.2024.109381.
[61] Letelier V, Hott F, Bustamante M, Wenzel B. Effect of recycled coarse aggregate treated with recycled binder paste coating and accelerated carbonation on mechanical and physical properties of concrete. J Build Eng 2024;82:108311. https://doi.org/10.1016/j.jobe.2023.108311.
[62] Ray S, Haque M, Sakib MN, Mita AF, Rahman MDM. Use of ceramic wastes as aggregates in concrete production: a review. J Build Eng 2021;43:102567. https://doi.org/10.1016/j.jobe.2021.102567.
[63] Higashiyama H, Yagishita F, Sano M, Takahashi O. Compressive strength and resistance to chloride penetration of mortars using ceramic waste as fine aggregate. Constr Build Mater 2012;26:96–101. https://doi.org/10.1016/j.conbuildmat.2011.05.008.
[64] Manikandan KP, Nanthakumar P, Balachandar M, Shankar DG, Vijayakumari G. Partial replacement of aggregate with ceramic tile in concrete. Mater Today Proc 2023. https://doi.org/10.1016/j.matpr.2023.05.214.
[65] Mistri A, Kumar S, Dhami N, Mukherjee A, Barai SV. A review on different treatment methods for enhancing the properties of recycled aggregates for sustainable construction materials. Constr Build Mater 2020;233:117894. https://doi.org/10.1016/j.conbuildmat.2019.117894.
[66] Varshney H, Khan RA, Khan IK. Quality improvement techniques for recycled aggregate concrete incorporating fibers and Bacillus species bacteria: a review. Mater Today Proc 2024. https://doi.org/10.1016/j.matpr.2023.03.223.
[67] Tavakoli D, Heidari A, Karimian M. Properties of concretes produced with waste ceramic aggregate. Asian J Civ Eng 2013;14:369–82.
[68] Reusing ceramic waste as fine aggregate and supplemental cementitious material in the manufacture of sustainable concrete. Constr Build Mater 2023.
[69] Phan QHN, Vo HT, Bui PT, Nguyen NT. Effect of Recycled Coarse Aggregate Treatment Using Cement – Sodium Bicarbonate Slurry on Compressive Strength of Hardened Concrete. Lecture Notes in Civil Engineering. 2022 Sep 21;449–57. https://doi.org/10.1007/978-981-19-3303-5_38
[70] Andal MN, Thenmozhi R, Bahurudeen A. Strength enhancement of recycled fine aggregate beam through chemical treatment – A waste to wealth approach. J Mater Res Technol. 2024;30:7340–7351. https://doi.org/10.1016/j.jmrt.2024.05.069
[71] Grabiec AM, Klama J, Zawal D, Krupa D. Modification of recycled concrete aggregate by calcium carbonate biodeposition. Construction and Building Materials. 2012;34:145–150. doi:10.1016/j.conbuildmat.2012.02.027
[72] Hamada HM, Shi J, Abed F, Al Jawahery MS, Majdi A, Yousif ST. Recycling solid waste to produce eco-friendly ultra-high performance concrete: A review of durability, microstructure and environment characteristics. Sci Total Environ. 2023;876:162804
[73] AFNOR. NF EN 933-1. Essais pour déterminer les caractéristiques géométriques des granulats – Partie 1. Paris: AFNOR; n.d.
[74] ASTM C29/C29M-07. Standard test method for bulk density (unit weight) and voids in aggregate. West Conshohocken (PA): ASTM International; 2007. https://doi.org/10.1520/C0029_C0029M-07.
[75] ASTM C128-22. Standard test method for relative density (specific gravity) and absorption of fine aggregate. West Conshohocken (PA): ASTM International; 2022.
[76] ASTM C20-00(2022). Standard test methods for apparent porosity, water absorption, apparent specific gravity, and bulk density of burned refractory brick and shapes by boiling water. West Conshohocken (PA): ASTM International; 2022. https://doi.org/10.1520/C0020-00R22.
[77] Tuan NH, Huynh LX, Anh PH. A fuzzy finite element algorithm based on response surface method for free vibration analysis of structure. Vietnam J Mech 2015;37:17–27. https://doi.org/10.15625/0866-7136/37/1/3923.

[78] Sun Q, Zhu H, Li H, Gao M. Application of response surface methodology in the optimization of fly ash geopolymer concrete. ISA Trans 2018;48:45–52.
[79] Arshad HM, Akhtar M, Gilmour SG. Augmented Box–Behnken designs for fitting third-order response surfaces. Commun Stat Theory Methods 2012;41:4225–39. https://doi.org/10.1080/03610926.2011.568154.
[80] Zhang L, Yue Y. Influence of waste glass powder usage on the properties of alkali-activated slag mortars based on response surface methodology. Constr Build Mater 2018;181:527–34. https://doi.org/10.1016/j.conbuildmat.2018.06.040.
[81] Myers RH, Montgomery DC, Anderson-Cook CM. Response surface methodology: process and product optimization using designed experiments. 3rd ed. Hoboken (NJ): John Wiley & Sons; 2009.
[82] Senthamarai RM, Manoharan PD. Concrete with ceramic waste aggregate. Cem Concr Compos 2005;27:910–3. https://doi.org/10.1016/j.cemconcomp.2005.04.003.
[83] Liu F, Liu J, Ma B, Huang J, Li H. Basic properties of concrete incorporating recycled ceramic aggregate and ultra-fine sand. J Wuhan Univ Technol Mater Sci Ed 2015;30:352–60. https://doi.org/10.1007/s11595-015-1152-3.
[84] Brunello V, Corti C, Sansonetti A, Tedeschi C, Rampazzi L. Non-invasive FTIR study of mortar model samples: comparison among innovative and traditional techniques. Eur Phys J Plus 2019;134:1–17. https://doi.org/10.1140/epjp/i2019-12667-1.
[85] Wolpert M, Hellwig P. Infrared spectra and molar absorption coefficients of the 20 alpha amino acids in aqueous solutions in the spectral range from 1800 to 500 cm^{-1}. Spectrochim Acta A Mol Biomol Spectrosc 2006;64:987–1001. https://doi.org/10.1016/j.saa.2005.08.025.
[86] García-González J, Rodríguez-Robles D, Wang J, De Belie N, Morán-del Pozo JM, Guerra-Romero MI, et al. Quality improvement of mixed and ceramic recycled aggregates by biodeposition of calcium carbonate. Constr Build Mater 2017;154:1015–23. https://doi.org/10.1016/j.conbuildmat.2017.08.039.
[87] Zerig T, Aidoud A, Belachia M, Djedid T, Abbas M. Combined sand eco-mortar reinforced with polyethylene terephthalate: behavior and optimization using RSM method. Constr Build Mater 2023;404:133160. https://doi.org/10.1016/j.conbuildmat.2023.133160.
[88] Boumaaza M, Belaadi A, Alshahrani H, Bourchak M, Jawaid M. Response surface methodology optimization of palm rachis biochar content and temperature effects on predicting bio-mortar compressive strength, porosity and thermal conductivity. J Nat Fibers 2023;20. https://doi.org/10.1080/15440478.2022.2162184.
[89] Zerig T, Belachia M, Aidoud A, Meftah N, Djedid T, Abbas M. Statistical analysis using the RSM approach of the physical behavior of green polymerized eco-mortar. J Clean Prod 2024;450:141858. https://doi.org/10.1016/j.jclepro.2024.141858.